



The Persistent Scatterer Interferometry (PSI) technique for ground deformation and landslide monitoring using Sentinel-1 images time-series

NATTIYA KORAWAT

A THESIS SUBMITTED IN PARTIAL FULFILLMENT OF
THE REQUIREMENTS FOR MASTER OF SCIENCE
IN GEOINFORMATICS
FACULTY OF GEOINFORMATICS
BURAPHA UNIVERSITY

2020

COPYRIGHT OF BURAPHA UNIVERSITY

เทคนิค Persistent Scatterer Interferometry (PSI) เพื่อวิเคราะห์การเสถียรของพื้นดินและพื้นที่ดินถล่มโดยใช้ภาพถ่าย Sentinel-1



ณัฐธิญา โคระวัตร

วิทยานิพนธ์นี้เป็นส่วนหนึ่งของการศึกษาตามหลักสูตรวิทยาศาสตรมหาบัณฑิต

สาขาวิชาภูมิสารสนเทศศาสตร์

คณะภูมิสารสนเทศศาสตร์ มหาวิทยาลัยบูรพา

2563

ลิขสิทธิ์เป็นของมหาวิทยาลัยบูรพา

The Persistent Scatterer Interferometry (PSI) technique for ground deformation and
landslide monitoring using Sentinel-1 images time-series



NATTIYA KORAWAT

A THESIS SUBMITTED IN PARTIAL FULFILLMENT OF
THE REQUIREMENTS FOR MASTER OF SCIENCE
IN GEOINFORMATICS
FACULTY OF GEOINFORMATICS
BURAPHA UNIVERSITY

2020

COPYRIGHT OF BURAPHA UNIVERSITY

The Thesis of Nattiya Korawat has been approved by the examining committee to be partial fulfillment of the requirements for the Master of Science in Geoinformatics of Burapha University

Advisory Committee

Examining Committee

Principal advisor

.....
(Professor Dr. Timo Balz)

..... Principal examiner
(Professor Dr. Shao Zhengfeng)

..... Member
(Professor Dr. Jianzhong Lu)

..... Member
(Professor Dr. Shi Lei)

..... Member
(Dr. Tanita Suepa)

..... Member
(Lecturer Dr. Pattama Phodee)

..... External Member
(Professor Dr. Orhan Altan)

..... Dean of the Faculty of Geoinformatics
(Lecturer Dr. Kitsanai Charoenjit)

This Thesis has been approved by Graduate School Burapha University to be partial fulfillment of the requirements for the Master of Science in Geoinformatics of Burapha University

..... Dean of Graduate School
(Associate Professor Dr. Nujjaree Chaimongkol)

61910098: MAJOR: GEOINFORMATICS; M.Sc. (GEOINFORMATICS)

KEYWORDS: Persistent Scatterer Interferometry (PSI), Permanent Scatterer (PS), Quasi-Persistent Scatterer (QPS), Ground deformation, Landslide, InSAR

NATTIYA KORAWAT : THE PERSISTENT SCATTERER INTERFEROMETRY (PSI) TECHNIQUE FOR GROUND DEFORMATION AND LANDSLIDE MONITORING USING SENTINEL-1 IMAGES TIME-SERIES.
ADVISORY COMMITTEE: TIMO BALZ, 2020.

This thesis focuses on the surface motion and landslide monitoring using remote sensing imagery. Landslides are among the most severe and unpreventable geomorphological hazards in the mountainous area. The monitoring and management of ground deformation are necessary for early warning systems. Satellite imageries are effective tools to study the ground deformation. The extraction of information from SAR (Synthetic Aperture Radar) images can provide changes on the Earth's surface. Displacement maps derived from SAR images show the displacement in the LOS (Line of Sight) direction of the satellite. This technique can provide the capabilities for measuring the deformation in high resolution with a precise accuracy of 1 millimeter/year.

The objectives of this research are to increase the potential of ground deformation monitoring leading to the identification of landslide using PSI and to compare the effectiveness of PSI in urban and rural areas.

This research demonstrates the methodology to overcome limitations of temporal and geometric decorrelation with repeat-pass satellite data using the Persistent Scatterer Interferometry (PSI), which is applied to investigate and monitor the ground deformation. Besides, PSI can increase the potential of ground deformation surveillance leading to the identification of landslides. The trend of ground deformation is obtained by using InSAR time-series analysis of Persistent Scatterer (PS) and Quasi-Persistent Scatterer (QPS) from Sentinel-1 SAR images acquired from 2017 to 2019. The advantages of Sentinel-1 SAR images are the open access and all-weather availability. The PS technique is used to explore stable point-like radar targets, which works well in urban areas. However, it has a limitation to be applied in heavily vegetated areas. The QPS technique is used to analyze in more

complex terrain, which can process the most coherence interferogram as a weight for each interferometric phase to improve the coherence target and the spatial distribution of QPS points within vegetated areas. These techniques have significantly applied to monitor the severity of deformation and landslide.

This thesis considers the research questions; How is the ground deformation derived from PSI processing to recognize stable and unstable areas? How effective is the PSI technique to detect ground deformation in urban and rural areas?

To answer these research questions, the Sentinel-1 SAR images were selected. The PSI approach was used to investigate the ground deformation and landslides in both city and rural areas. Beijing, China is capital of China and has been among the most seriously affected city by subsidence. Fangshan District in Beijing was selected due to the occurrence of a massive landslide. Another study area is Nan province located in northern Thailand where landslides occur every year, especially in the rainy season and most of the area in this province is a mountainous area covering with the heavy vegetation.

The results show displacement rates in Beijing city, with -99 to 19 mm/yr. There were two obvious displacements in the eastern part. The susceptible areas of Beijing were related to the geological structure, the density of buildings, and the distribution of infrastructure. One landslide in PS and two landslides in QPS were identified in Beijing rural case study; there were observed as slow-moving landslide with a motion of 5 mm/yr. The displacement map indicated that the QPS was also capabilities of detecting land deformation in Nan case study, with rate of -262 to 248 mm/yr. The most susceptible areas located on hilltops and steep valleys. The QPS results performed is better than the results of PS because they can improve the coherence and the measured points in high and complex terrain.

The displacement maps were generated using PS and QPS; it can be explained in the movement and identification of susceptible areas. The landslides were detectable using both techniques but probably undetectable during continuous monitoring with the PS in heavy vegetation areas. Any landslides loss in detect is a small landslide, located in a valley where no structures as potential good radar targets are reflectance. The results extracted by PS usually have the advantage of high

backscatter and stable phase. Thus, the displacement acquired by PS only refers to PS points, but the QPS can be detected the displacement in the area without PS points. The integration of different techniques is significantly advantageous for monitoring land deformation and landslides. However, both techniques will be useful for local development planning and decision making



ACKNOWLEDGEMENTS

I would like to appreciate my supervisor Prof. Dr.-Ing Timo Balz for accepting me as his student. I am very grateful for all support, guidance, comment to make this research a success. I am grateful to my co-advisor Dr. Tanita Suepa for suggestions, advice, and recommendations to the end of my research; Dr.Pattama Phodee for advice and suggestion in SAR acknowledgment, encouragement, and concern for all students. I also would like to Steve McClure for guiding the knowledge in research methodology and Scientific writing lectures. Thanks to Daniele Perissin, who is the developed software of Sarproz for processing multi-temporal InSAR data and the Sarproz team for support and guidance to complete my research.

I would like to grateful teachers of the State Key Laboratory for Information Engineering in Surveying, Mapping and Remote Sensing (LIESMARS), teachers of the School of International Education at Wuhan University, and staff of the Geo-Informatics at Burapha University for their support from the beginning of Master studies.

I really appreciate the Geo-Informatics and Space Technology Development Agency (GISTDA), who has supported Sirindhorn Center for Geo-Informatics (SCGI) scholarship for giving me an opportunity to have a good experience.

A very special thanks to my family for always encouraging me. Thanks to all my friends and SAR group members for helping and sharing knowledge and many wonderful moments.

Nattiya Korawat

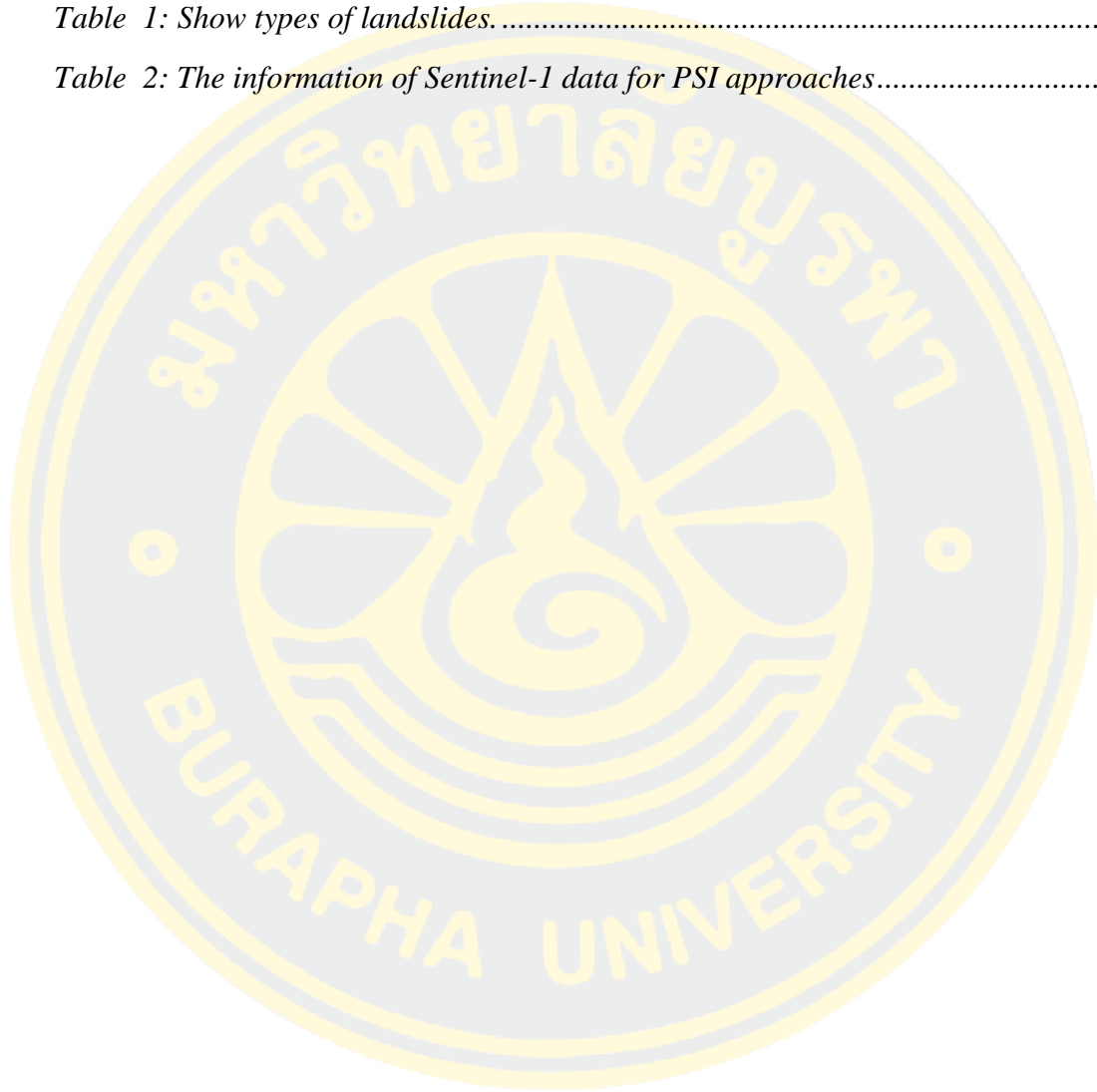
TABLE OF CONTENTS

| | Page |
|--|-------------|
| ABSTRACT..... | D |
| ACKNOWLEDGEMENTS..... | G |
| TABLE OF CONTENTS..... | H |
| LIST OF TABLES..... | J |
| LIST OF FIGURES..... | K |
| CHAPTER I..... | 1 |
| INTRODUCTION..... | 1 |
| 1.1. Statement of the problem..... | 1 |
| 1.2. Scope of study..... | 4 |
| 1.3. Research question..... | 5 |
| 1.4. Objective..... | 5 |
| 1.5. Definition of terms..... | 6 |
| 1.6. Thesis structure..... | 7 |
| CHAPTER II..... | 8 |
| LITERATURE REVIEW..... | 8 |
| 2.1. Ground deformation..... | 8 |
| 2.2 Definition of landslides..... | 9 |
| 2.3 Remote Sensing monitoring and management..... | 13 |
| 2.4 Synthetic Aperture Radar (SAR)..... | 14 |
| 2.5 Synthetic Aperture Radar Interferometry (InSAR)..... | 17 |
| 2.6 Persistent Scatterer Interferometry (PSI)..... | 21 |
| 2.6.1 Persistent Scatterer (PS)..... | 24 |
| 2.6.2 Quasi - Persistent Scatterer (QPS)..... | 25 |
| 2.7 Landslide monitoring..... | 26 |
| CHAPTER III..... | 29 |

| | |
|---|----|
| METERAIL AND METHODOLOGY | 29 |
| 3.1 Study area | 29 |
| 3.1.1 Beijing Municipality, China | 29 |
| 3.1.2 Nan province, Thailand | 31 |
| 3.2 Data..... | 34 |
| 3.3 Method..... | 38 |
| 3.3.1 Persistent Scatterer (PS) | 39 |
| 3.3.2 Quasi-Persistent Scatterer (QPS)..... | 40 |
| CHAPTER IV | 44 |
| RESULTS | 44 |
| 4.1 Ground deformation velocity map from PSI processing | 44 |
| 4.1.1 Persistent Scatterer (PS) | 44 |
| 4.1.2 Quasi-Persistent Scatterer (QPS)..... | 51 |
| 4.2 Landslide identification | 58 |
| 4.3 Connection graph of PS and QPS processing..... | 60 |
| 4.3.1 Temporal coherence estimation..... | 60 |
| 4.3.2 Connection graph of temporal coherence..... | 62 |
| CHAPTER V | 65 |
| CONCLUSION AND DISCUSSION | 65 |
| 5.1 Conclusion | 65 |
| 5.2 Discussion..... | 66 |
| 5.3 Limitation and recommendation..... | 69 |
| REFERENCES | 70 |
| BIOGRAPHY | 78 |

LIST OF TABLES

| | Page |
|--|-------------|
| <i>Table 1: Show types of landslides.....</i> | 10 |
| <i>Table 2: The information of Sentinel-1 data for PSI approaches.....</i> | 35 |



LIST OF FIGURES

| | Page |
|--|-------------|
| <i>Figure 1: The landslides occurred on a mountainous area (a) Nan, Thailand on July 28th, 2018 (b) Nan, Thailand on May 16th, 2017 (c) Beijing on August 11th, 2018 (d) subsidence in Beijing on February 16th, 2014.</i> | 5 |
| <i>Figure 2: The result of ductile deformation curves.</i> | 9 |
| <i>Figure 3: Show the major types of landslide movement</i> | 12 |
| <i>Figure 4: The Electromagnetic (EM) Spectrum</i> | 14 |
| <i>Figure 5: The simplified geometry of a synthetic aperture radar system.</i> | 16 |
| <i>Figure 6: The geometry of (a) ascending and (b) descending satellite orbits.</i> | 16 |
| <i>Figure 7: The spaceborne SAR missions</i> | 17 |
| <i>Figure 8: The data of DEM or DSM and DTM</i> | 19 |
| <i>Figure 9: The study area in Beijing, China</i> | 30 |
| <i>Figure 10: Geological structures of study area in Beijing, China</i> | 31 |
| <i>Figure 11: The study area in Nan, Thailand</i> | 32 |
| <i>Figure 12: Geological structures of the study area in Nan, Thailand</i> | 34 |
| <i>Figure 13: The statistical information of the dataset in PS analysis. (a) Beijing, (b) Nan.</i> | 35 |
| <i>Figure 14: The dataset of Sentinel-1 SAR images in the PS technique (a) PS technique in Beijing (city and rural) with 62 total number of SAR images. (b) PS technique in Nan with 68 total number of SAR images.</i> | 36 |
| <i>Figure 15: The statistical information of the dataset in QPS analysis. (a) Beijing, (b) Nan.</i> | 37 |
| <i>Figure 16: The dataset of Sentinel-1 SAR images in the QPS technique (a) The rural area of Beijing with 62 total number of SAR images. (b) Nan Province with 77 total number of SAR images.</i> | 37 |
| <i>Figure 17: The conceptual framework for PSI processing</i> | 41 |
| <i>Figure 18: The ground deformation velocity map in Beijing city case study with PS analysis, The color bar range of -100 to 100 mm/yr.</i> | 45 |

| | |
|--|-----------|
| <i>Figure 19: The serious displacement centers are observed in Chaoyang and Tongzhu district, overlay on Google Earth.</i> | <i>46</i> |
| <i>Figure 20: The displacement patterns using the PS analysis</i> | <i>47</i> |
| <i>Figure 21: The ground deformation velocity map in Beijing rural case study with PS analysis, The color bar range of -20 to 20 mm/yr.</i> | <i>48</i> |
| <i>Figure 22: The serious displacement centers are observed along the road and building in the Mentougou district.....</i> | <i>49</i> |
| <i>Figure 23: The ground deformation velocity map in Nan case study with PS analysis, the color bar range of -20 to 20 mm/yr.....</i> | <i>50</i> |
| <i>Figure 24: The displacement map of PS analysis along LOS direction, overlay on Google Earth in the Nan, Thailand.....</i> | <i>51</i> |
| <i>Figure 25: The ground deformation velocity map in Beijing rural case study with PS analysis, the color bar range of -50 to 50 mm/yr.</i> | <i>52</i> |
| <i>Figure 26: The displacement patterns using the QPS analysis. The color bar ranges from – 50 to 50 mm/yr.....</i> | <i>54</i> |
| <i>Figure 27: The ground deformation velocity map in Nan case study by QPS analysis, color bar range of -100 to 100 mm/yr.</i> | <i>55</i> |
| <i>Figure 28: The displacement map focus on high-velocity rates, overlay on Google Earth.</i> | <i>55</i> |
| <i>Figure 29: The displacement patterns using the QPS analysis. The color bar ranges from – 100 to 100 mm/yr.....</i> | <i>57</i> |
| <i>Figure 30: The one landslide has been detected, located near Mixi road in Fangshan district.</i> | <i>58</i> |
| <i>Figure 31: The two landslides have been detected. These landslides located in Fangshan district (a) and (b) Yuta road.....</i> | <i>59</i> |
| <i>Figure 32: The temporal coherence estimation in Beijing city case study with PS analysis</i> | <i>61</i> |
| <i>Figure 33: The temporal coherence estimation of PS processing. (a) Beijing rural, (b) Nan case study.....</i> | <i>61</i> |
| <i>Figure 34: The temporal coherence estimation of QPS processing. (a) Beijing rural, (b) Nan case study.....</i> | <i>62</i> |
| <i>Figure 35: The connection graph in Beijing city case study with PS analysis.....</i> | <i>63</i> |

| | |
|--|----|
| <i>Figure 36: The connection graph in Beijing rural case study. (a) PS analysis, (b) QPS analysis</i> | 63 |
| <i>Figure 37: The connection graph in the Nan case study. (a) PS analysis, (b) QPS analysis</i> | 64 |
| <i>Figure 38: The displacement maps where the road detection with PS analysis in Beijing city case study</i> | 66 |



CHAPTER I

INTRODUCTION

This work investigates the ground deformation for the identification of landslides using a method known as the Persistent Scatterer Interferometry (PSI). This chapter describes the research problem, the scope of the study, the research questions and objectives, the definition of terms, and outlines the thesis structure.

1.1. Statement of the problem

Landslides are among the most severe and unpreventable geomorphological hazards in mountainous areas. The monitoring and management of ground deformation are necessary for the early warning system in community prevention. Deformation is a movement in the subsurface that investigates to landslides, which have an impact on the environment and can cause casualties. The increase of human activities and natural phenomena, e.g., deforestation, land-use changes, rapid urbanization, highway construction, extreme soil erosion, and rainfall, are triggering factors for landslides to occur. Moreover, the landslide inventory is also important information for risk management. Usually, this information is based on the interpretation of aerial photos and ground surveys; which may spend a lot of time and cost to collect and manage them. In addition, the data quality also depends on the efficiency of the operator. Remote Sensing data can provide various necessary information for assisting the disaster monitoring, which can significantly improve its quality by using SAR interferometry. Therefore, satellite imageries are powerful tools to precise the ground deformation measurement, leading to identify the possible landslide that can be a process repeated at different time intervals and available at various scales.

The Synthetic Aperture Radar Interferometry (InSAR) can offer a great support to natural hazard detection and monitoring. The InSAR time-series analysis, an indispensable solution to several works in environmental science, can measure the displacement information on the Earth's surface monitoring. Sentinel-1 SAR images are available under almost all-weather conditions. This image has widely used to monitor the displacements and prepare the warning systems issue, important for a

disaster mitigation perspective. Taking the differences of the phase measurements from the InSAR images achieved at two different points in time is very useful for understanding the movement of ground deformation trends indicating susceptibility areas.

This research demonstrates the methodology to overcome the limitation of temporal and geometric decorrelation with repeat-pass satellite data using advanced technique of SAR Interferometry as the Persistent Scatterer Interferometry (PSI), successfully applied by several researchers to geohazards monitoring, e.g., earthquakes, subsidences, velocities, volcanic eruptions, and landslides. PSI techniques can significantly increase the potential of ground deformation measurement, leading to the identification of a landslide, which has occurred in the recent past and is probable to occur in the future. Moreover, the PSI-derived deformation velocity rate can separate between stable and unstable areas. Therefore, these approaches have been used for deformation time series analysis of PSI processing, such as Persistent Scatterer (PS), and Quasi-Persistent Scatterer (QPS). Sentinel-1 images acquired from 2017 to 2019 have been used to an analysis by the Sarproz software implementation on Matlab software.

The advantage of the PSI in the InSAR technique is to overcome the limitations of geometric and spatial-temporal decorrelation. The main goals of PSI processing are the generation of single master stack interferograms and removal of topographic phase, selection of PSC based on amplitude stability index, estimation and removal of atmospheric phase screen using PSC, and finding additional PS points. The main PSI components improved; the selection of pixel increased the density and quality of PSI measurements such as the distribution of scatterers and the partial coherence target; the phase unwrapping algorithms; the using of flexible and increasing accuracy of the deformation models; estimation of the atmospheric phase component; the potentiality to generate large-site deformation analysis. Due to several limitations, the efficiency of the PSI significantly decreases, such as the high deformation velocity rate, lack of human-made structure, and topographic characteristics. The accuracy of the PSI technique depends on several factors. These factors including the distance from a reference point, the number of radar images, the time span of images, the coherence,

and even the sensor. This can provide the capabilities for high resolution measuring the deformation and precise accuracy of 1 millimeter/year.

The Persistent Scatterer (PS) focuses on exploring stable point-like radar targets (A. Ferretti, Prati, & Rocca, 1999). This method works well in urban areas, but it is difficult to be applied in heavily vegetated areas, and the number of permanent scatterers is low. The PS technique is not suitable for the mountain area, which prominent to the number of detected points is not enough to achieve accurate results of deformation. However, the condition of vegetation, steep slope, normal baseline, and time repeat pass of the satellite, cause less detection of PS target because of the low coherence.

The Quasi-Persistent Scatterer (QPS) is usually applied for the detection and monitor of ground deformation in heavily vegetated areas that overcome the problem on the distribution of backscatterer to improve the spatial distribution of QPS points (Perissin & Wang, 2012). QPS combines both analysis of phase spatial and temporal correlation and is used to analyze the complexity of the terrain. Additionally, the QPS technique can process the most coherence interferogram as a weight for each interferometric phase and can improve the coherence target. To improve the coherence target, main components of the image graph are modified: firstly, the connectivities of an image that possibility of unwrapping the phase time-series, secondly, the connection number of each image, and thirdly, the goodness quantify as the weight of coherence to each link of images.

The potential of PSI for landslides monitoring has been investigated by many researcher, e.g., landslides (Bianchini et al., 2013; Del & Idrogeologico, 2012; Hilley, Bürgmann, Ferretti, Novali, & Rocca, 2004; Tofani, Raspini, Catani, & Casagli, 2014; (Nengwu et al., 2012), subsidence (M. Chen, Tomás, Li, Motagh, Li, & Hu, 2016), and velocity ground motion (Lagios et al., 2013). Few of the studied areas are unsuccessful in identifying the landslide because of the lack of buildings, steep mountains, and densely vegetated areas (Yarmohammad Touski, Veiskarami, & Dehghani, 2019; Andrew Hooper, Zebker, Segall, & Kampes, 2004)

1.2. Scope of study

In purpose, productive of the PSI can be rapidly analyzed to detect and monitor surface deformation with SAR images. These techniques have significantly increased the monitoring of landslide applications that provides valuable information for landslide activity assessments. The completion of this research is to obtain the deformation over the study area to analyze the deformation trend to identify the susceptibility of the area to landslides.

For the study of deformation in both rural areas and the city of Beijing, China and Nan, Thailand, the PSI method was used. The city of Beijing is the main business city of China. It is one of the most water-stressed cities in the world due to the water-overexploitation, such as industrial, household, and highway construction. It has been among the most severely affected cities by subsidence, building construction, and rapid urbanization (Yang et al., 2018). The PS was a suitable choice for this area because of the many existing human-made structures in an urban environment. Fangshan District in Beijing occurred a massive landslide on August 11th, 2018; a massive landslide was falling over a mountain road and temporarily interrupted the traffic flow.

Nan is a province located in northern Thailand, where landslides occur every year, especially in the rainy season. For example, on July 28th, 2018, six houses were impinged by the landslides, which also interrupted the traffic and caused eight deaths casualties. Hence, the QPS is the suitable choice for both Fangshan and Nan because most of these areas are the mountainous area covered with the heavy vegetation. The cases of the landslide are shown in figure 1.



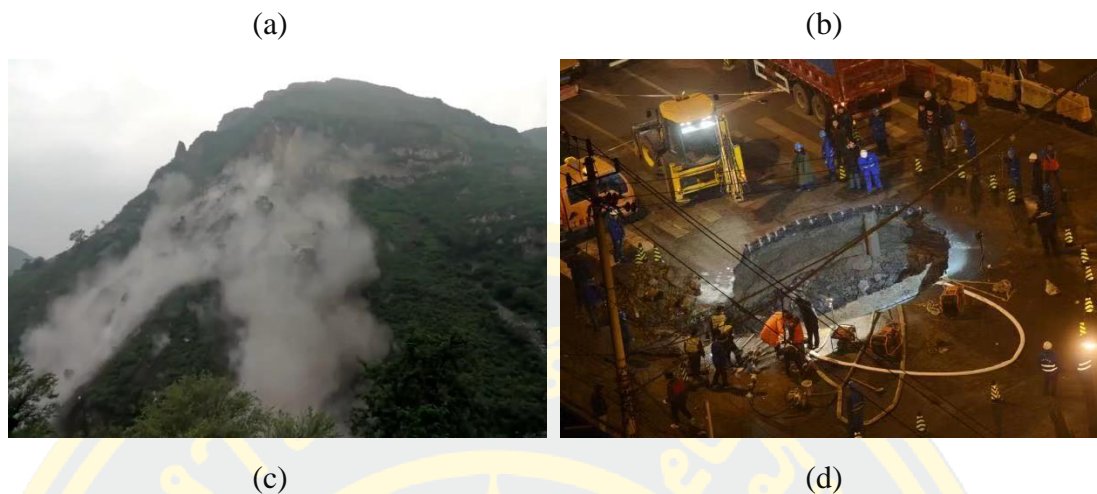


Figure 1: The landslides occurred on a mountainous area (a) Nan, Thailand on July 28th, 2018 (b) Nan, Thailand on May 16th, 2017 (c) Beijing on August 11th, 2018 (d) subsidence in Beijing on February 16th, 2014.

1.3. Research question

To get into more detailed analysis during the works on this research have to be challenged by answering the research question.

1. How is the ground deformation derived from PSI processing that recognizes stable and unstable areas??
2. How effectiveness is the PSI technique to detect ground deformation in the urban and rural areas?

1.4. Objective

This research focuses on the analysis of PSI approaches with open data and a commercial software. During the investigation of ground deformation and landslide monitoring in urban and non-urban areas, the capabilities and limitations will become increasingly obvious. The aim of the research is as follows:

1. To increase the potential of ground deformation leads to the identification of the landslide using PSI approaches.
2. To comparison effective of the PSI approaches in city and rural areas.

1.5. Definition of terms

The definition of terms is an explanation meaning of a word or expression that has described meaning in this research.

Coherence is meaning to the amplitude of the complex correlation coefficient of two SAR images.

DEM means points are characteristic of the shape of the bare-earth terrain without any objects, e.g., trees, buildings, roads.

Ground deformation is meaning to the change or any activity of an area of the surface causing the size, shape, or volume changes.

InSAR means to an effective way to measure changes in the land surface.

Landslide is meaning to the activity of mass wasting, includes a vast area of ground movements. The landslide occurs when the slope undergoes some process that changes its condition from stable to unstable.

PS meaning of the technique focuses on stable radar targets.

PS candidates or PSC meaning to the selection of scattered points based on amplitude stability index.

PSI meaning to an advanced technique of InSAR, which overcome limitations of spatial-temporal and geometric decorrelation.

QPS meaning of the technique improved the number of detected points.

Risk is meaning to the severity of deaths, persons injured, and harm to property or interruption of the economy due to the event.

SAR means to a radar system that is an active microwave remote sensing. Measuring the phase difference between a radar wave emitted from an antenna to a satellite or aircraft to generate high-resolution images.

Satellite image is meaning to the number of types of digitally transmitted images by artificial satellites were orbiting the Earth or other planets.

Sentinel-1 is meaning to the satellites designed to provide the spatial data for disaster, environment, security warranting, global economic, and business. The satellites are to operate day and night time, and perform with a synthetic aperture with radar imaging.

Velocity meaning to the rate of changes of deformation, measuring by PSI approaches.

1.6. Thesis structure

The advanced technique of Persistent Scatterer interferogram (PSI) is significantly to measure the ground deformation. The information is useful for local development to monitor and manage areas with a risk of natural disasters. It also serves researchers in further work.

This research is divided into five chapters. Chapter one is an introduction of the problem to the reason for the research, scope of the study, research question, objective, definition of terms, and outline research on thesis structure. Chapter 2 provides a brief overview of ground deformation, landslide monitoring, land subsidence, Remote Sensing monitoring, SAR, and InSAR application. Review of related literature describes the previous research focuses on the measurement tools to analysis ground deformation, landslide monitoring, the effectiveness and limitations of PSI technique in various sites. Chapter three describes the material and methodology. It includes the general of the study area, the dataset, and the PSI conceptual framework that is divided into three sections: pre-processing, preliminary analysis and geocoding, and InSAR processing. Chapter four contains experiment results of PSI for ground deformation trend measuring in city and rural areas of Beijing and Nan with accurate millimeter/year, connection graph in a different technique of PS and QPS. It also contains a comparison with reported software results and analyzes in detail. Chapter five provides a summary of the research and suggestions for future work.

CHAPTER II

LITERATURE REVIEW

This chapter provides the definitions, approaches, results, and limitations of previous research. The remote sensing monitoring application has presented the Synthetic Aperture Radar Interferometry (InSAR). The main methods are used to investigate ground deformation and landslides, which known technically as Persistent Scatterer Interferometry (PSI). This will be discussed thoroughly in this chapter.

2.1. Ground deformation

The ground deformation is a motion of subsurface material; it caused by a change of volume at a certain depth (Laat, 1996). This resulting in the topographic changing, such as subsiding, tilting, or forming bulges. Deformation is a process of the Earth's crust that affects the size, shape, or volume of the land. The characteristics of ground deformation occurrence depend on the type of rock and stress going into an area of the Earth's crust.

Deformation refers to a change in the shape or size of the target. Permanent deformation is irreversible even after the removal of the applied forces, while the temporary deformation is recoverable as it disappears. Temporary deformation is also called the elastic deformation, while the permanent deformation is called the plastic deformation. meanwhile, the rock bread under stress is called brittle deformation and the ductile deformation is folded or bent of subsurface without breaking. Its result is curved that can see in the rock shown in figure 2-1.

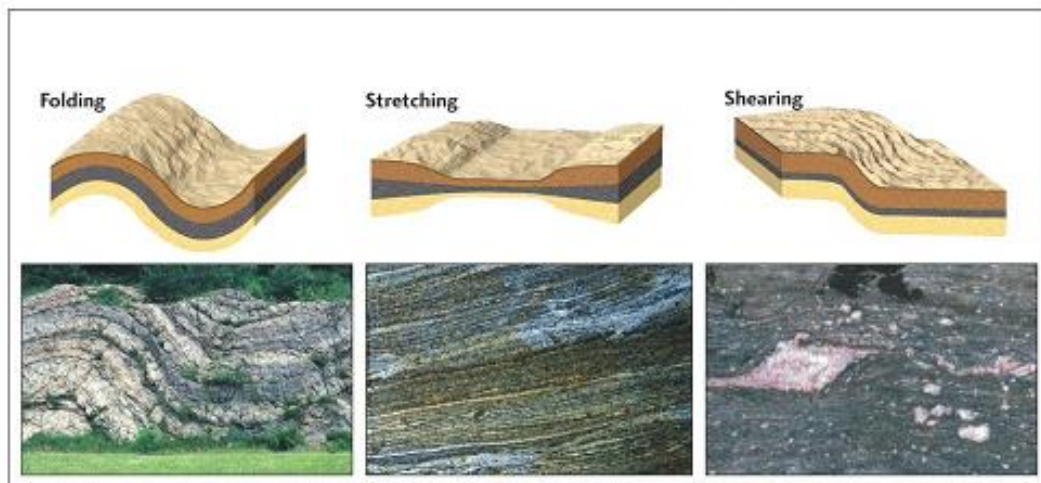


Figure 2: The result of ductile deformation curves.

(Source: <https://study.com/academy/lesson/what-is-deformation-definition-types-process.html>)

2.2 Definition of landslides

A landslide is defined as the motion of debris, rock, mudflows, or soils, which refers to downslope motion of them beneath the influence of the gravity. The landslide consists of five types of movement as falls, flows, slides, spreads, and topples further subdivided by type of their geological material as bedrock, debris, or earth. The landslide debris flows collectively referred to mudflows or mudslides, and rockfalls are a regular pattern of landslide types. Slope movement occurs when the force is acting down-slope, gravity, exceeds the strength of the earth materials combined to a slope. Furthermore, an earthquake and other factors are able to induce underwater landslides called the submarine landslides, which sometimes cause tsunamis damaging to coastal environments.

There are many aspects causing the landslide such as human, morphological and geological aspects. Geological factors include weathered, jointed or fissured material, sheared, adversely orientated discontinuities, permeability and material contrasts, earthquakes, snowfall, and rainfall. On the other hand, erosion, slope angle, slope loading, rebound, uplift, and vegetation changes are the morphological causes. Last, the human aspects pertain to the deforestation, excavation, loading, water management, land use (e.g., building, railway, road), mining and quarrying, vibration, and pollution.

Landslide can cause flooding by forming landslide dams that block valleys and streams. This causes subsequent downstream the flood happens when the dam fails, also solid landslide debris accumulated to streamflow, which cause channel blockages and diversions forming flood conditions or erosion. The various types of landslides are able to divide by properties of the material involved and the movement pattern that classifies the slope movements (Varnes, 1978) shown as table 1. Usually, landslide causes there are the following reasons for geological, morphological, and human causes.

Table 1: Show types of landslides.

| Type of movement | Type of material | | |
|-----------------------|--------------------------------|----------------------|--------------------|
| | Bedrock | Engineering soil | |
| | | Predominantly coarse | Predominantly fine |
| Falls | Rockfall | Debris fall | Earthfall |
| Topples | Rock topple | Debris topple | Earth topple |
| Slides | Rotational Rockslide | Debris slide | Earth slide |
| | Translational | | |
| Lateral spread | Rock spread | Debris spread | Earth spread |
| Flows | Rock flow | Debris flow | Earth flow |
| Complex | Rock flow | Debris flow | Earth flow |
| | (deep creep) | (deep creep) | (deep creep) |

The schematics represent the primary type of landslide movements, as following in figure 3: The most common types of landslides described as follows.

1. Two major types of slides are the rotational slides and the translational slide that are separated by the slide material from the more stable underlying material. The rotation slide is a movement of the surface of rupture curve concave upward, and casually rotating that is frequently to the surface and transverse across the slide (figure 3A). On the contrary, the translational slide is a slide along a casually planar surface with slight rotation or backward tilting (figure 3B). A block slide is one of the

translational slide which the moving mass consisting of a single unit or a few units move downslope as a relative mass (figure 3C)

2. Falls are the sudden movement of rocks and boulders that become detached from steep slopes or cliffs (figure 3D). Separation occurs with discontinuities such as fractures, joints, and bedding planes, and movement takes place by free-fall, bouncing, and rolling.

3. Topples are distinguished by the forwarding rotation of a unit about some pivotal point, below a unit, under the actions of gravity and forces exerted by close units or by fluids in cracks (figure 3E)

4. Flows are five basic types that diverge from one another in a primary.

4.1 Debris flow is a rapid mass movement which causes by the excessive water flow of the surface due to heavy rainfall or rapid snowmelt, erosion and concentrate soil or rock on steep is nearly saturated and consist of a large form of silt and sand-sized material (figure. 3F).

4.2 Debris avalanche is a category of extremely rapid debris flow (figure. 3G).

4.3 Earthflow has a sandglass shape (figure. 3H). The material liquefies and runs out, forming a bowl or depression at the head. The flow is stretch and commonly occurs in fine-grained materials or clay-bearing rocks on moderate slopes and under saturated conditions, although dry flows of granular material are also realistic.

4.4 Mudflow, which is one of earthflow that includes material that is wet enough to flow rapidly, and contains at least 50 percent of sand, silt, and clay-sized particles. Mudflows and debris flow usually mentioned to mudslides.

4.5 Creep is the slow, steady, downward movement of slope-forming soil or rock. The movements caused by shear emphasize enough to produce permanent deformation, but it is so small to produce shear failure (figure 3I).

5. Lateral spread is dominant because usually occur on flat terrain or gentle slopes (figure 3J). The predominant kind of movement is a lateral extension regulated by shear or tensile fractures. The failure happens when solid transforms to a liquefied state. Failure usually triggered by rapid ground motion that starts suddenly in the small areas and spreads rapidly.

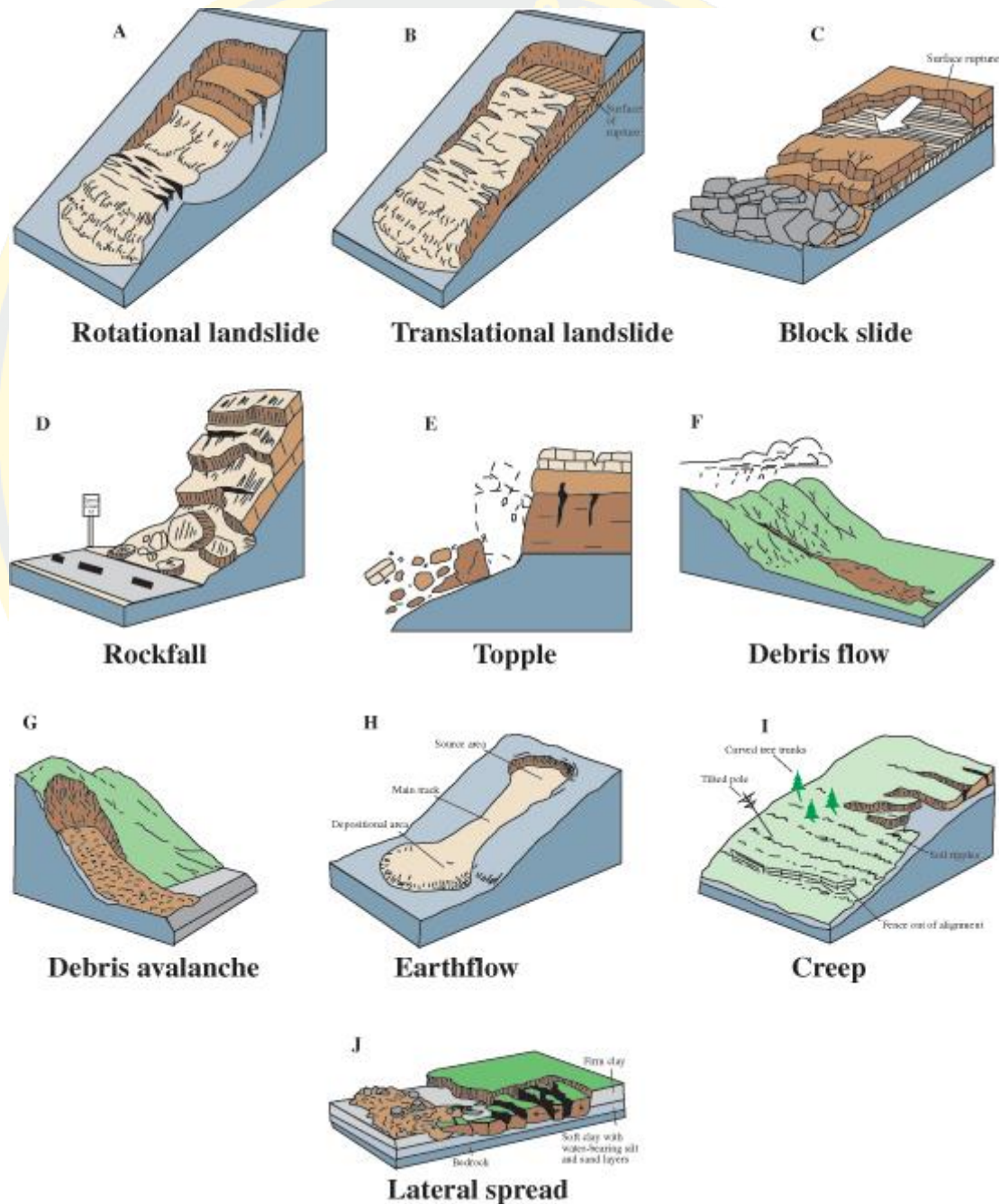


Figure 3: Show the major types of landslide movement
(Source: <https://pubs.usgs.gov/fs/2004/3072/fs-2004-3072.html>)

2.3 Remote Sensing monitoring and management

Remote sensing can be defined as observing without having any contact, which is essential to monitor and integrate various phenomena. Therefore, land surface deformation which is the change of the ground due to topographic changes (Dehghani & Javadi, 2013). These are one of the prominent phenomena associates with earthquakes, subsidence, landslide, and anthropogenic event (Otukey, Atolere, Gidudu, & Martini, 2019). The ground deformation is useful for understanding the behavior of a natural disaster (Safari, Gamse, & Seyedrezaei, 2018). Landslides are a natural disaster that can be triggered directly by natural and human activities caused by the deformation (Kincal et al., 2017). The development application of deformation extends into unstable areas within the increasing of human and natural activities become the important triggering factors for landslide occurrence (Zhang, Wang, & Xia, 2012).

Conventional geodetic techniques to monitoring the ground displacement include global positioning system (GPS) devices, leveling, and bedrock and layering mark surveying. These techniques determine the displacement on a point by point with high precision, but the measurement is difficult to obtain, the monitoring range is small, and the cost is high (Strozzi, Wegmüller, Tosi, Bitelli, & Spreckels, 2001). Besides, the remote sensing data have been well utilized, such as airborne light detection and ranging (LiDAR), spaceborne synthetic aperture radar (SAR), ground-based SAR, optical sensors, and terrestrial LiDAR, with surveying measurements and observations. They have been the success in the generation of landslide inventory, landslide deformation, and landslide susceptibility (Zhao & Lu, 2018). Hence, Remote Sensing (RS) and Geographical Information Systems (GIS) analysis are a significant role in landslide zonation. Moreover, the identification of landslide is important data for the landslide assessment, which can be effective, particularly on image processing (Reddy & Reddy, 2014).

Remote sensing images are powerful tools to measure landslide displacement, and are able to process repeatedly at different time intervals and various scales. This application can detect and measure the ground movements within a short time period to monitor phenomena by using SAR data (Blasco, Foumelis, Stewart, & Hooper, 2019).

2.4 Synthetic Aperture Radar (SAR)

Synthetic Aperture Radar (SAR) is the system of an active microwave image, which provides its illumination and operation that returns the echo from radar pulses to generate an image. Furthermore, neither clouds, fog, nor precipitations have a significant effect on microwave systems, thus permitting all-weather imaging (Vant, 1989).

SAR systems emit the electromagnetic (EM) waves and collect the returned backscatter reflecting from a target in the antenna look direction. The EM spectrum is the entire range of energies that are produced as a result of the interaction between matter and energy. The stages of the spectrum are distinguished with considered to the wavelength; gamma rays, X-rays, ultraviolet rays, visible light, infrared rays, radar, FM, TV, shortwave, and AM shown as figure 4.

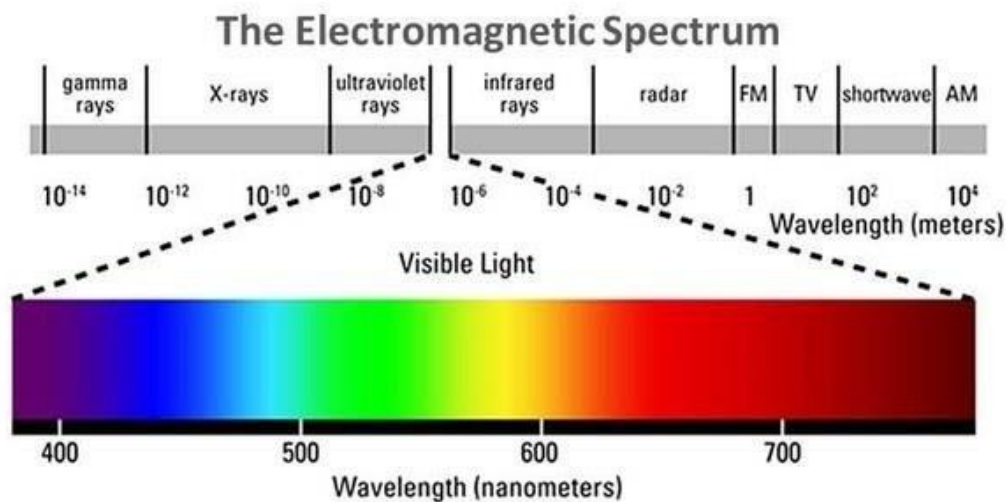


Figure 4: The Electromagnetic (EM) Spectrum

(Source: <http://mydeliciousmoments.com/deliciousness-of-loving-light-healing%E2%99%AA/>)

The radar systems emit the coherent radiation in the microwave portion of the spectrum. EM radiation has a sinusoidal radiation pattern with amplitudes going through well-defined minimum and maximum. Each wavelength (space of two peaks) corresponds to 360° and the unit distance is defined by wavelength to measure the SAR phase. SAR measurements have two observables as amplitude and phase. The amplitude is the power of the backscattered EM wave, and links to the target, orientation, and electrical properties (Osmanoğlu, Sunar, Wdowinski, & Cabral-Cano, 2016).

SAR receiver detects the stream of echoes reflected from the surface. The energy scattered back towards the radar is called backscatter, and the echoes are produced since the terrain consists of different scatterers such as, trees, rocks, or buildings on the surface that interact with the incoming microwave radiation. So, the phase and amplitude return signals depending on the backscatter characteristics of the target. The received signals are complex, having both amplitude and phase. The received amplitude is characterized by geometrical properties of the scatterer, as well as geometrical imaging factors. Also, the received phase is determined by the phase of the transmitted signal, the dielectric properties of the medium, and the position of the scatterer. The SAR focused image, referred to the single-look complex (SLC), is arranged in a 2D array with coordinates slant range for the length from SAR and azimuth for the location of the scatterer along a flight pathway shown as figure 2-4. High signal-to-noise ratio (SNR) is desirable in all radar systems. To increase the pulse energy of SAR which focuses on transmitting a linear frequency modulated (FM) chirped pulse and allows the usage of longer pulses

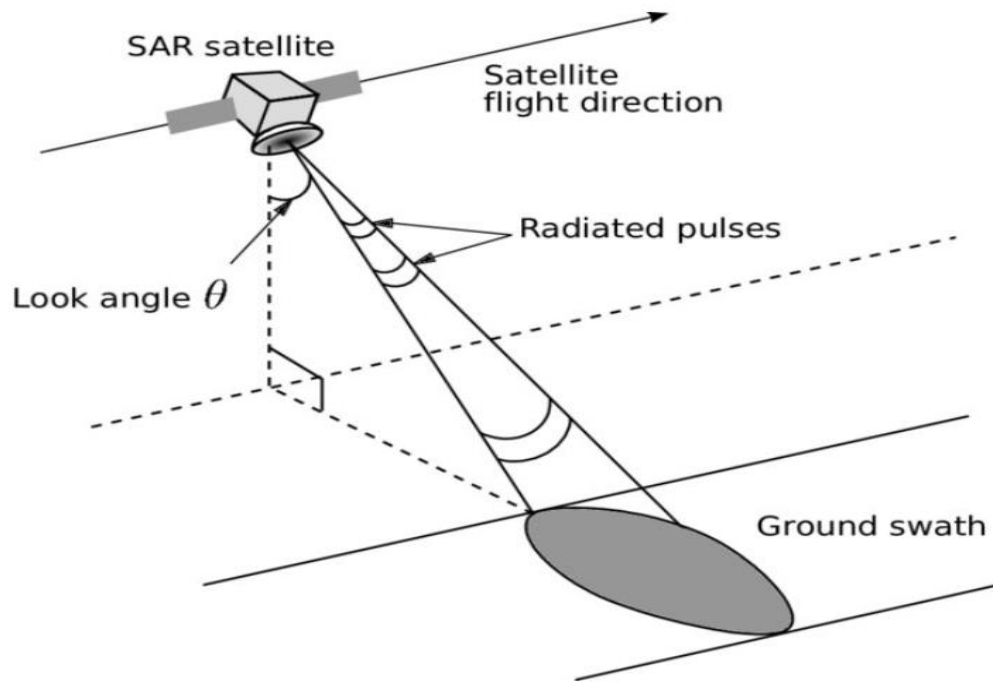


Figure 5: The simplified geometry of a synthetic aperture radar system.

The satellite orbit passes area in both ascending and descending directions crosses the equator. An ascending orbit is defined where the satellite path is going from south-north. On the contrary, the descending orbit where the satellite path is going from north-south, shown as figure 6.

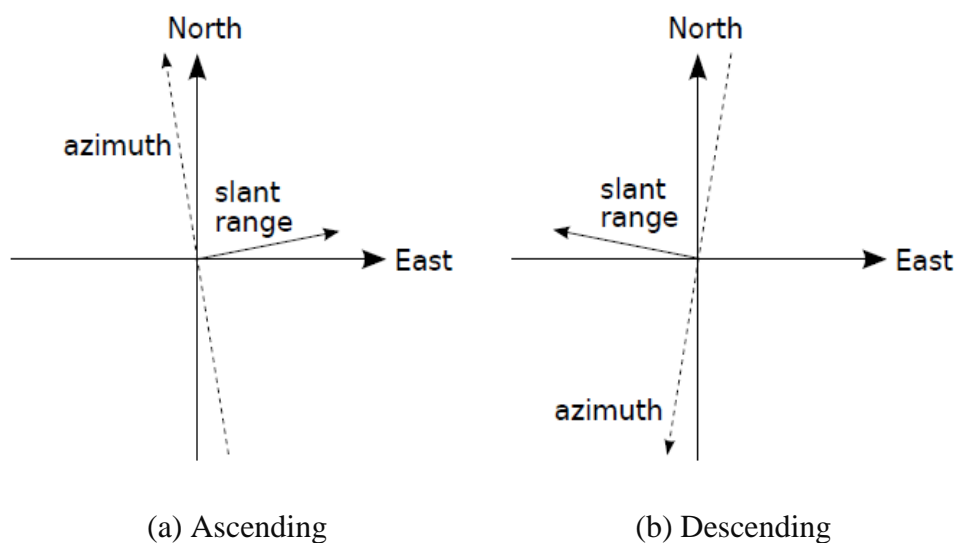


Figure 6: The geometry of (a) ascending and (b) descending satellite orbits.

Since the European Space Agency (ESA) has launched the satellite in the early 1990s. The subsequent acquisition of continuous SAR images over a given time span, radar interferometry has been effectively used to measure the Earth's topography with millimeter-scale surface displacement (Pope, Rees, Fox, & Fleming, 2014). The Sentinel-1 (C-band) has launched with a wavelength between 4cm – 8cm, the spaceborne SAR missions shown as figure 7:

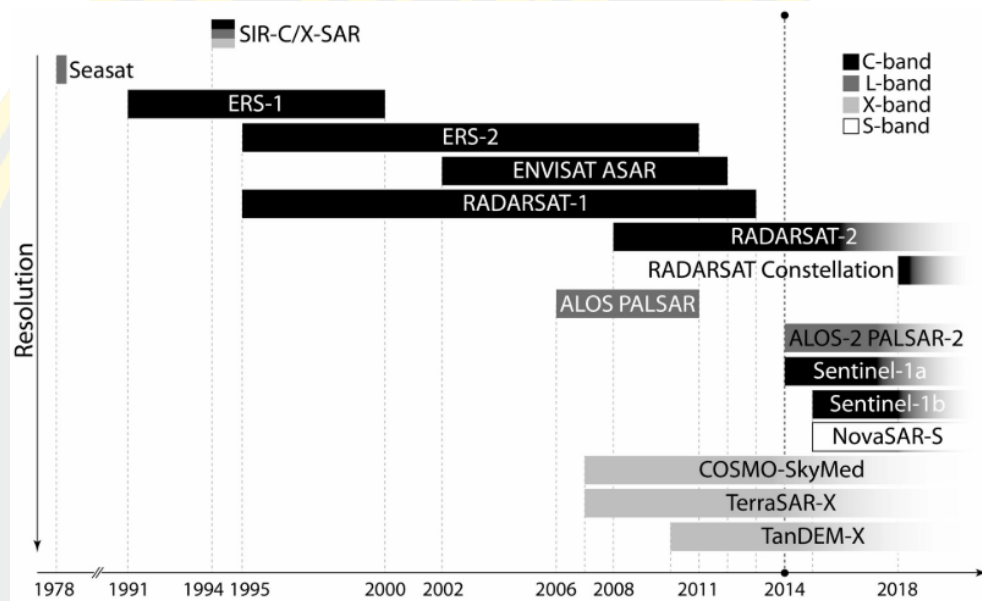


Figure 7: The spaceborne SAR missions
(Source: Pope, Rees, Fox, & Fleming, 2014)

2.5 Synthetic Aperture Radar Interferometry (InSAR)

Synthetic Aperture Radar Interferometry (InSAR) has been applied to measure changes on the earth's surface in the early 1990s. In particular, InSAR can offer the great support to natural hazard detection, and monitoring tool to measure change on the Earth's surface analysis. Additionally, the InSAR measurements are mainly sensitive to terrain, surface motions, atmospheric conditions, spatial separation of satellites, and the electrical properties of the ground. So, there are multiple types of collecting Interferometric data.

The single-pass interferometry is the primary approach in which a satellite carries two antennas, one antenna takes both the transmitter and receiver, but another antenna holds only the receiver. The distance between antennas called the

interferometric baseline, which results in a low error when it detects the elevation of the target. The other type is the repeat-pass interferometry, which carries only one antenna acting as both transmitter and receiver. The satellite needs to travel two times over the target and to minimize error of the target elevation. Therefore, it seems that the repeat-pass interferometry has high complications. Owing to the purpose of the satellite is to monitor phenomena like in the case of landslide investigation, then this process becomes advantageous. Consequently, the repeat-pass interferometry can be performed under the condition that the image targets remain coherent. Decorrelation is a loss of coherence due to the phase is being interfered. In addition, this technology has advantages in monitoring the land deformation of all-weather, large-scale, high-precision, and complex terrain (K. Zhou, Wang, Wang, & Ding, 2019).

The atmospheric noise is the differential path length excess in slant range and contaminates the InSAR measurement. Moreover, the magnitude of the atmospheric effects can have a high temporal change by cause of the distribution of water vapor in the troposphere. (Nathan & Scobell, 2012). The errors in DEM directly result in phase error in topographic residuals in cases where perpendicular baselines are quite large. Incorrect orbit information result in the errors of the interferometric baseline. Additionally, the errors in the baseline generate phase noise spatially correlated and appeared as phase ramps across the differential interferogram. The interferometric phase can solve the errors to estimate a refined baseline.

Spatial and temporal decorrelation are the two most significant sources of decorrelation noise. The geometric change causes the spatial decorrelation divided into volumetric and baseline decorrelation. The volumetric decorrelation originates from the scatterers distribution that cumulative backscatter arising from propagation and interaction of the signal with the targets within the resolution cell depends on the angle at which the target is imaged. Also, the baseline decorrelation is caused by the differential of the SAR geometry in the secondary image concerning with the reference image. Thus, to decrease the spatial decorrelation noise, the special standard bandpass filters used to reduce the range bandwidth and range resolution, which produces the coherent. Moreover, the shot of perpendicular baselines should be used to pairs the SAR

images. In contrast, the backscatter properties changes in the surface over time between observations causes to the temporal decorrelation (Zebker & Villasenor, 2007).

The most important applications of the InSAR techniques are Digital Elevation Models (DEM) and ground deformation monitoring (Rosen, 2000). Digital Elevation Model (DEM) represents the bare earth surface without any objects such as plants, trees, and buildings. DEM, which is often used in geographic information systems, is the most common basis for digitally-produced relief the maps shown as figure 8.

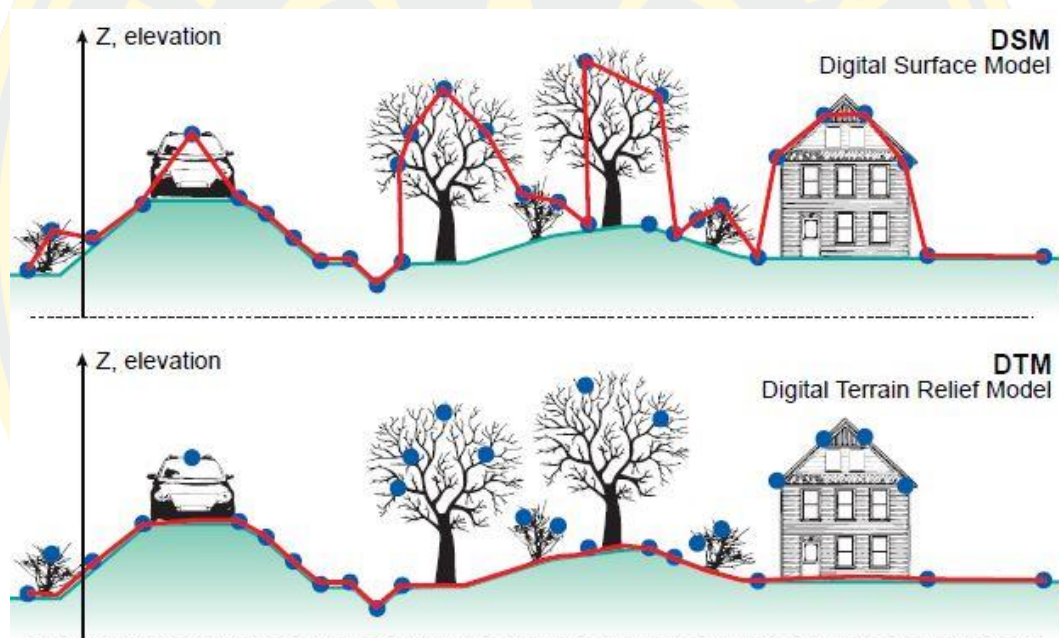


Figure 8: The data of DEM or DSM and DTM
(Source: <http://www.charim.net/datamanagement/32>)

The ground deformation is measured by interferogram with the range changes that affect the phase difference between two acquisitions of radar phase images (X. Zhou, Chang, & Li, 2009). The InSAR techniques have been successfully used to monitor moving landslides and the landslide inventory is an important information because the damaged areas located in the higher velocity tend to occur new landslide (Francisca & Javier, 2015). Usually, landslide inventory is interpreted based on aerial

photo interpretation and field surveys; however, it is time-consuming, high-cost, and data quality depend on the experience of the operator. Hence, Remote Sensing data can be significantly improved the data quality by SAR interferometry (Notti, Meisina, & Zucca, 2009). Moreover, the Interferogram also allows accurate measurements of the displacements of radar targets along the satellite line of sight (LOS) direction. Measurement with computed the differentiation of phase values of two synthetic aperture radar (SAR) images gathered at different times over the same area of interest (Perissin & Rocca, 2006). Several researchers using radar images investigated the ground displacements (Crosetto, Monserrat, & Budillon, 2019). The spatial density and uncertainties of displacement are estimated because it is important for the interpretation of motion.

Several limitations of this technique can reduce the accuracy of the results due to the Atmospheric Phase Screen (APS), the residual topographic contributions, and the decorrelation effects (Bozzano, Mazzanti, Perissin, Rocca, & De Pari, 2017). In addition, the repeat-pass interferometry can be affected by the atmospheric effect, which is one of the most intractable problems. The radar signals may suffer from the propagation delays when it travels through the atmosphere. So, the atmospheric state can be vary considered among the acquisitions.

The main limitations are related to the temporal and geometric decorrelation that cause a loss in the coherence and prevent to derive the measurement in each pixel (Plain et al., 2016). The temporal decorrelation stems from the changes in natural terrain, anthropogenic, weather conditions, which occur when the distribution of wavelength-scale scatterers. Conversely, the geometric decorrelation consisted of variation in reflectivity of the targets as layover, foreshortening, and shadowing on SAR images. It is the result of a difference in an incidence angle between the two sensors (Emardson, Simons, & Webb, 2003). Nonetheless, the advanced techniques which are sufficient to reduce some of the limitations are provided by multi-interferometric so-called Persistent Scatterer Interferometry (PSI).

2.6 Persistent Scatterer Interferometry (PSI)

In order to overcome limitations of spatial-temporal and geometric decorrelation with repeat-pass satellite mode, the PSI becomes to the advance of the InSAR technique (Greif & Vlcko, 2013) as the Persistent Scatterer Interferometry (PSI). PSI focuses on exploring point-like radar targets (A. Ferretti et al., 1999). Thus, these techniques work well in urban areas, but it is difficult to be applied in heavily vegetated areas (Luo, Perissin, Dogan, Lin, & Wang, 2012). In contrast, the Quasi-Persistent Scatterer (QPS) analysis are used to the complex terrain, which works well in non-urban areas, given available dataset and weight each interferometric by using the best subset (Perissin, Wang, Prati, & Rocca, 2013a). Small BAse Line Subset: SBAS are used to generate the deformation in large scales, but it not suitable to detect the local and small scales (Berardino et al., 2002). They are successfully applied by several researchers in geohazards monitoring, e.g., landslides (Bianchini et al., 2013, Del & Idrogeologico, 2012), subsidence (M. Chen, Tomás, Li, Motagh, Li, Hu, et al., 2016), velocity ground motion (Lagios et al., 2013).

The main of PSI processing are; generation of single master stack interferograms and removal of topographic phase, PSC selection based on amplitude dispersion index, estimation and removal of atmospheric phase screen using PSC, and finding additional PS points.

Firstly, the generation of the single master stack interferograms and removal of the topographic phase from each interferogram that is important for high information to use a small baseline. To avoid the effects of temporal decorrelation, moreover, geometric decorrelation interferes with distributed scatterers. Thus, a large baseline will affect registration and pixels containing PS points will remain coherent.

Secondly, the amplitude dispersion index selects the Persistent Scatterer Candidates (PSC) based on the scatterer amplitude value, defined as the standard deviation ratio. The idea applied to a strong scatterer (high amplitude), and a weak scatterer (low amplitude), the phase change due to the noise at the same level will be much less in the strong scatterer. The pixels correspond to pixels, whose coherence is dominated by a single point scatterer.

Thirdly, calculate the Atmospheric Phase Screen (APS), which starts with the estimation of the master images; all interferograms can be estimated by an average of the residual. The spatial network is formed using PSC. After APS estimation, all unwanted signals removed from the observation and DEM error, then scatterer velocity can be calculated on a phase value for each PSC (Alessandro Ferretti, Prati, & Rocca, 2001).

The interferometric phase signal, $\Delta\phi_{int}$, is the results of multiple contributions, that indicate the following terms (Massonnet & Feigl, 1998):

$$\Delta\phi_{int} = \Delta\phi_{topo} + \Delta\phi_{displ} + \Delta\phi_{atmo} + \Delta\phi_{noise} \quad (1)$$

Where $\Delta\phi_{topo}$ is the contribution of residual topographic height after the DEM subtraction from an interferograms. $\Delta\phi_{displ}$ is searched for displacement information. $\Delta\phi_{atmo}$ is the disturbance caused by Atmospheric Phase Screen (APS). $\Delta\phi_{noise}$ is the non-removable phase disturbance.

The main PSI components improved; the selection of pixel increased the density and quality of PSI measurements such as distributed scatterers and partially coherence targets; the improvements of phase unwrapping algorithms; the use of more flexible and accurate deformation models; the improvements to estimating the atmospheric phase component; the ability to generate large-area deformation analysis (Crosetto, Monserrat, Cuevas-González, Devanthery, & Crippa, 2016).

Deformation velocity in the landslides is commonly used in the component measured along the line of sight (LOS), which separates the area of stable and unstable (Oliveira, Zêzere, Catalão, & Nico, 2015). The distribution of PS obviously depends on the reflectivity and temporal coherence characteristics of objects on the earth's surface (Fiaschi, Holohan, Sheehy, & Floris, 2019). However, the one limitation of the spatial density of PS point is coherent that it can provide hundreds of PS per square kilometers in urban areas and a few points in vegetated areas (Perissin & Wang, 2012). Efficient of PS in urban areas where human-made constructions are increased the feasibility

generation of stable scatterer better than in non-urban areas (Höser, 2018). The coherence refers to PS and human-made structure, but less correspond in non-urban areas, deformation velocity rate alternative used may not be sufficient in complex areas in case of landslides (Carlà, Raspini, Intrieri, & Casagli, 2016). High backscatter in human-made structure with proper coherence where natural terrain incapable reflects backscatter from the object (Kincal et al., 2017).

PSI and SBAS can be identify areas where the surface affected by geometric and temporal decorrelation. Both techniques are identified as a homologous coherence of 85% in the urban areas (Carlà, Raspini, Intrieri, & Casagli, 2016). It can resolve the deformation of low coherence, able to delineate the border of deformed areas, but unable to detect an object on vegetation areas (Heimlich et al., 2015). SBAS is modified to detect ground deformation whole significantly in the regional and local scale that coherence is preserved in a limitation portion, mostly in urban areas (Guzzetti et al., 2009). Building and human-made structures do not correspond while most of PS points identified over non-urban areas in shorter repeat time by significant LOS displacement (Alessandro Ferretti, Colesanti, Perissin, Prati, & Rocca, 2004) additionally, these techniques are effective in detecting slope movement in vegetated areas and also densely urbanized area by the generation of deformation time-series analysis (Kuri, Arora, & Sharma, 2018). The effect on InSAR found that temporal decorrelation is an important problem in heavily vegetated areas and also the atmospheric effects are very significant at times. Thus, the InSAR technique can be used effectively to monitor the ground displacement in flat and less built-up areas, but the steep mountain and high building present some difficulties to be applied (Ding, Liu, Li, Li, & Chen, 2004).

The accuracy of the PSI technique depends on several factors. These factors include the length from a reference point, the number of radar images, the time span of images, the coherence, and even the sensor. The PSI can provide the capabilities for high resolution for measuring the deformation and precise accuracy of 1 mm/yr (A. Hooper, Segall, & Zebker, 2007). The several limitations, such as high deformation velocity rate, lack of man-made structure and topographic characteristic, causing to the efficiency of the PSI significantly decreases (Yarmohammad Touski et al., 2019).

Although the PSI offers a way to reduce the main limitations in the conventional InSAR method, there are still several disadvantages to this technique. First, it needs many SAR images as possible to analyze the ground deformation. Second, not all buildings can be observed by the PSI. Third, the PSI is not suitable for monitoring the densely vegetated areas because of too low PS density (Andrew Hooper et al., 2004).

2.6.1 Persistent Scatterer (PS)

The PS technique involves interferometric phase comparison of SAR images, gathered at different times and with different baselines (A. Ferretti et al., 1999) precise accuracy to the millimeter for terrain deformation and meter for DEM. Accuracy depends on the size of the images stack was used to estimate statistical of the amplitude, also used Persistent and distribution scatterer. This technology removes the residual topographic component of the flattened interferogram phase for each PS points, then unwrapping the PS phases both spatially and temporally. The method finds the stable scatterers independent of amplitudes associated with man-made structures. It is suitable in areas where conventional InSAR fails due to complete decorrelation of the majority of scatterers, but a few stable scatterers are presented (Andrew Hooper et al., 2004).

In order to overcome limitations are induced by time interval, especially in non-urban areas given a low incidence that is good for an estimate to accurate the result (Patrascu, Popescu, & Datcu, 2016). PS analysis, the interferometric phase is generated by referring all slave images to a common master image (Perissin & Wang, 2011) to extract the information from a partially coherence target. The PS relies on the analysis of a backscattered signal from co-registrations, multi-temporal SAR images to identify highly reflective ground deformation, that is stable from an electromagnetic point of view (Ciampalini, Raspini, Lagomarsino, Catani, & Casagli, 2016). Moreover, in the mountainous area covered with dense vegetation during different seasons influence high noise, PS reduced and precise this information (Chang, Yen, Hooper, Chou, & Chen, 2010). However, the problem of heavy vegetation cannot be improved with PS technique, but PS performs better in urban areas than in natural terrain (Vöge et al.,

2015). Most PS points are identified where a human-made structure and residential areas (Luo et al., 2012).

Thus, the method was suitable for monitoring of the urbanized area, where the density of PS is higher (Ciampalini et al., 2014). In contrast, the PS technique is not suitable in the non-urban area because the less images in the mountain area and the number of PS points are required to achieve more precise deformation results (Mi et al., 2017).

2.6.2 Quasi - Persistent Scatterer (QPS)

The QPS technique is high performance to detect ground deformation, which can extract information from the partially coherent target as the weight of phase estimation (M. Gao et al., 2019). This technique is used to relax the strict conditions imposed by PS analysis. In order to extract deformation from coherent targets and to improve the spatial distribution of measurement points (Perissin & Wang, 2012). QPS technique combined analysis of phase spatial and temporal correlation (Kuri et al., 2018), which applied to the monitoring of ground deformation in the vegetation area and also improved the number of detected points (Razi, Sumantyo, Perissin, & Kuze, 2018). So, it is appropriate for an area where the density of permanent scatterer is not high (H. Chen et al., 2018), e.g., in the complex terrain changes and the low number of available images (Perissin, Wang, Prati, & Rocca, 2013b).

The limitation of spatial density detected of PS point (hundreds of PS per km^2 in an urban area, a few points in vegetated areas) has been improved significantly by QPS that allows extract the information from the coherent target (Wang et al., 2010). The spatial distribution of QPS points is similar in both agricultural and residential areas (Luo et al., 2012).

2.7 Landslide monitoring

In general, there are four methods of analysis involve landslides (Edwin L. Harp, 2008). First, the geotechnical model concerning quantitative methods, analysis of engineering slope stability to evaluate the relationship between the thickness of the soil layer on various slopes and the water level in the changing soil mass. The uncertainties are unusually high or low, and to estimate the hazard of the probability fail of the hill through the direct application of calculation techniques with the factor of safety (Kim et al., 2004). Second, the geomorphic analysis represents the first step to create the inventory, which is quantitative methods. Analyzing the topography or morphology obtained by field surveys or visual interpretation from aerial photos and satellite images to assess the location of landslide susceptibility (Hansen, 1984). Third, the weight parameter analysis represents weighting and rating various factors that are determined by expertise, which is a qualitative analysis (Baum, Galloway, & Harp, 2008). Fourth, the statistical analysis is an analytical analysis method that can analyze one or two variables to compare each factor or analyze multiple variables to describe a quantity. It influences landslide or density distribution. It is a quantitative analysis (Edwin L. Harp, 2008).

The spatial distribution of landslide risk obtained by spatial subdivision of the area under the conditions and multiplication of spatial landslide probability, affected zones, land-use, population, property, and vulnerability (Leone et al., 1996). The seasonality of landslides is obviously occurred in rainy seasons and obtain temporary stability in dry seasons. The landslide located on sides of the valley and rivers with a slope that is higher than 25° , account of 90% of all landslides. The main factors inducing landslides are artificial cutting of slopes, as well as side erosion by ditches and rivers (J. Gao & Sang, 2017). Rainfall is the elementary triggering factor agent for landslides and frequently used to slope failures prediction. However, the relationship between the rainfall and landslide occurrence is relatively complicated, but there is no widely accepted method for rainfall-induced landslide prediction (S. Bai., 2013).

The landslide could be considered eligible to investigate and monitor for predict, more frequently in case of landslides increasing overtime by ground displacement. A large amount of displacement information can be obtain for several

areas of the world by PS interferometry (Del & Idrogeologico, 2012). These information presents the displacement occurrence in the rates of a slow-moving landslide (Hilley et al., 2004). The PSI technique based on long series, number of images, more accurate the results of co-registration, multi-temporal SAR imagery.

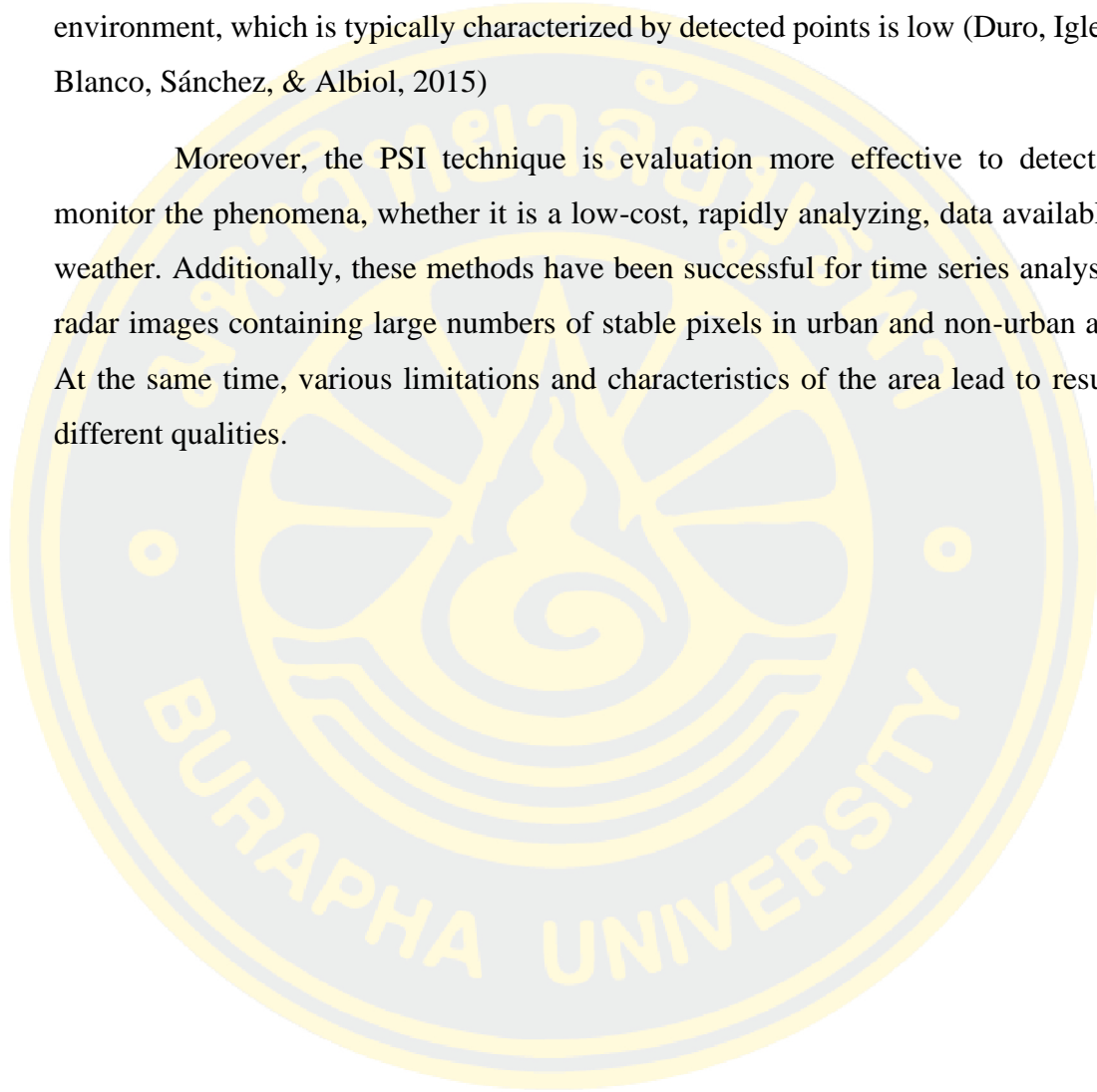
The time-series analysis are better understanding of the deformation pattern and its relations with the cause of landslide itself, which are suited to define the landslides, ground motions, and responses to triggering factors (Tofani et al., 2014). SAR images time-series allows the Atmospheric Phase Screen (APS) estimation to reduce the effect of the atmosphere in the displacement measurement (Roque, Fonseca, Henriques, & Falcão, 2014). Due to the time series analysis on PS pixels, it can reduce the decorrelation effect, orbital error, and DEM error, atmospheric delay, etc., monitor landslide with deformation rate map represent several new landslides areas (Nengwu et al., 2012).

The advanced technique of InSAR are significantly applied to monitor the severity of deformation and landslide that demonstrate valuable information in landslide activity assessments. The landslide pattern and ground instability were identified by multi-temporal images (Bozzano et al., 2017). Ground subsidence is the main causes of geological hazard that divide into two groups as the natural and human-induced subsidence. Thus, the natural subsidence mainly includes deformations of soft soil and geomorphological fail, while the human-induced subsidence caused by water overexploitation, land reclamation, underground mining, and concentrated construction (Ding et al., 2004).

Sentinel-1 images are used for routine monitoring of displacements, with the opportunity to prepare warning systems issues such as the increase of subsidence due to groundwater pumping that may yield into the formation of sinkholes or a slope activity causing for landslide incidence (Lazecky et al., 2016). Besides, the PS product are also exploited to define the state of geohazard activity and update pre-existing geohazard inventory. In order to offers beneficial data for risk management, widely recognized for ground displacement monitoring, whole vast areas in a timely and cost-efficient way (Yang et al., 2018). The displacements are measured considering a reference point of known coordinates (Ciampalini, Raspini, Frodella, et al., 2016).

PSI processing are used to improving the monitoring of landslide. The results of this technique are demonstrated the improvement of both the density and quality of the displacement rate. This technique is the main factor in landslide monitoring applications. Commonly, the effect on temporal decorrelation occurs in the natural environment, which is typically characterized by detected points is low (Duro, Iglesias, Blanco, Sánchez, & Albiol, 2015)

Moreover, the PSI technique is evaluation more effective to detect and monitor the phenomena, whether it is a low-cost, rapidly analyzing, data available all weather. Additionally, these methods have been successful for time series analysis of radar images containing large numbers of stable pixels in urban and non-urban areas. At the same time, various limitations and characteristics of the area lead to result in different qualities.



CHAPTER III

METERAIL AND METHODOLOGY

In order to accomplish the research, was described the characteristics of the study area, the dataset, and the methodology. The study area was selected in Beijing, China and Nan, Thailand. The data of Sentinel-1 SAR images were used to analyze the trend of deformations. The conceptual framework was divided into three sections; pre-processing, preliminary analysis and geocoding, and InSAR processing.

3.1 Study area

In purpose, specifying the various site in city and rural areas to increase the capabilities of ground deformation, also to landslide monitoring. Three study areas, including city and rural of Beijing, China and Nan province, Thailand.

3.1.1 Beijing Municipality, China

Beijing municipality located in northern China, with 16 urban, suburban, and rural districts, which an area of 16,807 square kilometers. The terrain is high in western to northern, but low in southern to eastern. The elevations range from 60 to 80 above mean sea level in the front of the mountains, 20 to 60 mean sea level in the plains.

Beijing is the central business city of China, which is one of the most water-stressed cities in the world due to the overexploitation of water, such as industrial, infrastructure. Since 1950, it has been among the most severely affected by land subsidence, rapid urbanization, and building contracture. The mainly cause by the excessive withdrawal of groundwater, sub-way excavation, and controlled by lithological & geological structure. The sudden sinking of the ground caused by a natural event, removal of water, oil, or mineral resources, ground pumping requires 3.5 billion liters/year to supply more than 20 million people. The reduction of the land surface observed in the city and downtown due to loss support beneath the ground, causing subsidence. Moreover, the increases of land subsidence due to groundwater pumping into the formation of sinkholes or a slope activity that might be causing a landslide incidence. In western Beijing is a mountainous area by the Taihang

mountains. This area occurred the massive landslide in Fangshan district on August 11th, 2018, and another landslide was observed from Google Earth. For this reason, a case study was determined in both the city and rural areas of Beijing using PS and QPS technique shown in figure 9.

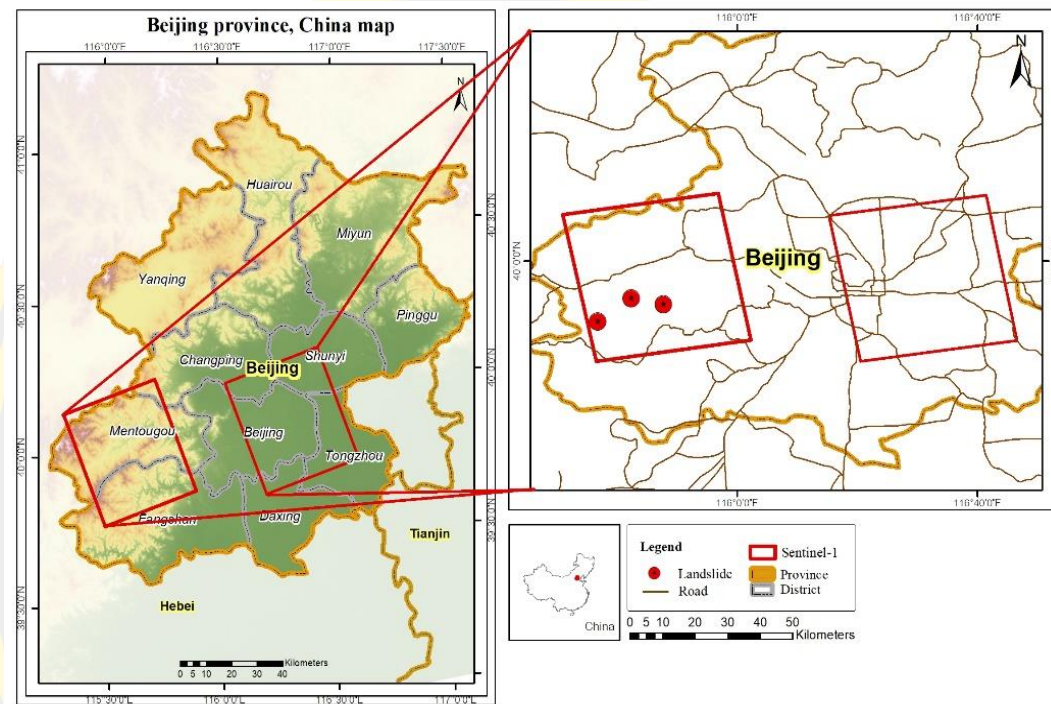


Figure 9: The study area in Beijing, China

Geological characteristics of the Beijing study area were shown on a regional map (modified from <http://portal.onegeology.org/OnegeologyGlobal/>). Beijing plain in eastern is composed of sedimentary rocks as Quaternary, while a mountain in western is composed of intermediate and sedimentary rocks, volcanic rocks, and intermediate grade metamorphic rocks. Beijing city was formed by Quaternary sediments transported of main rivers, which the main component of Quaternary sediment is clay, intervened by sand with groundwater. Apart from Beijing rural in western, most of the landslides occurred in the sedimentary rock. Landslides occurred mainly along the hill where the road cuts were highly weathering rock mass; also slope instability causes landslide typologies. A geological map appears in this case study, as shown in figure 10.

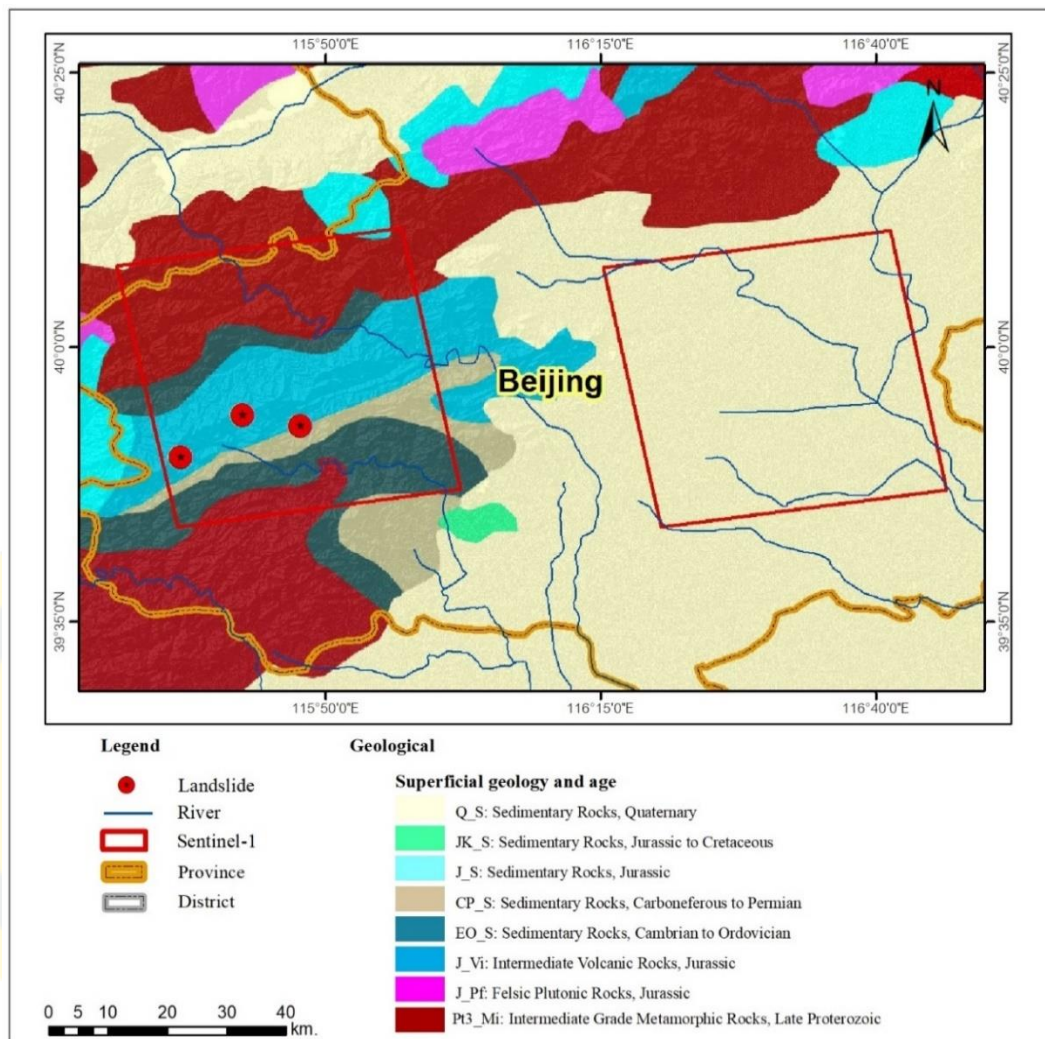


Figure 10: Geological structures of study area in Beijing, China (Modified from <http://portal.onegeology.org/OnegeologyGlobal/>)

3.1.2 Nan province, Thailand

Nan province located in northern Thailand, at coordinates 18.7756° N, 100.7730° E, with 15 districts, 99 sub-districts, 890 villages, which an area of 12,163 square kilometers. The terrain is high, which is steep mountains, approximately 85% of the province. The Phlueng Range is in the western part and the Luang Prabang Range is in the eastern, northeast of Nan towards the border with Laos. Doi Phu Kha mountain is the highest of 1,980 meters. The elevation ranges from 600 to 2000 meters above mean sea level, slope exceeding 30 degrees.

The spatial distribution of the villages is a direction along the valley, river, and road, which are severely affected by the natural disaster in the rainstorm season, e.g., landslide, mudslides, and immerse flood. Usually, the landslide in Nan province occurs every year; there is an impact on the environment, property, and human life. During a few decades, Nan has affected a tropical cyclone and low pressure for several days in the rainy season, which causes frequent phenomena to this area, e.g., the landslide on July 28th, 2018, six houses impingement by landslides, which also interrupted the traffic and caused eight deaths. For this reason, the northern part of Nan was selected, as shown in figure 11.

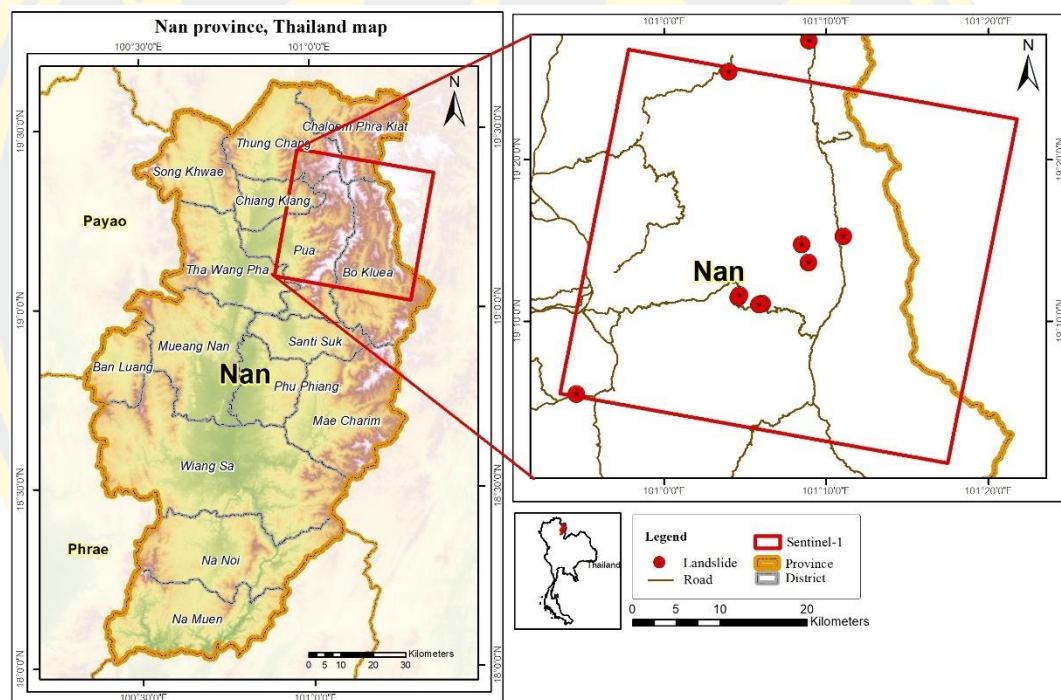


Figure 11: The study area in Nan, Thailand

The topography consists of highland and mountainous areas. A number of watersheds have been formed due to the flow of several rivers. The riverbank has become a fertile ground for farming and settlement.

The geological structures of the Nan case study are sedimentary and metamorphic rocks. Mountain in the eastern is composed of conglomerate, Sandstone, Shale, and mudstone. This is a great influence on rock decay, especially for areas at

active fault due to water and air passing through a gap of rock layers. The decay of rocks depended on physical and chemical properties. It is the most important factor influencing the occurrence of landslides. Most of the landslides occurred in the sedimentary rock, which is higher weathering and erosion, also a triggering factor as rainfall-induced saturated soil and sensitive water presence. Phenomena can occur in forms of intense rainfall, ground-water levels changes, and water-level changes along coastlines, dams, and the banks of lakes, reservoirs, canals, and rivers. A geological map appears in this case study, as shown in figure 12.

1. Qa is Fluvial deposits: gravel, sand, silt, and clay of channel, riverbank, and flood basin.

2. Tmm is Semi-consolidated claystone and siltstone, red to brownish red; lignite, calcareous claystone, mudstone; ligneous claystone with calcareous parting, gastropods, fish, ostracods; conglomerate, sandstone, white to light gray, moderately sorted; shale, light.

3. Ksk is siltstone, sandstone, purple, red to brownish red, and red with Calcrete horizons.

4. JKpw is Quartzitic sandstone, white, pink, and gray, large scale cross-bedded, thick-bedded, intercalated conglomeratic sandstone; thin laminations of red siltstone; claystone.

5. Tr2 is shale, chert, thin-bedded; and limestone, with *Halobia* sp., *Daonella* sp., and radiolaria.

6. PTr is sandstone, tuffaceous sandstone, argillaceous limestone, meta-rhyolitic tuff, meta-andesitic tuff, shale, limestone lens, chert, and oncolitic limestone.

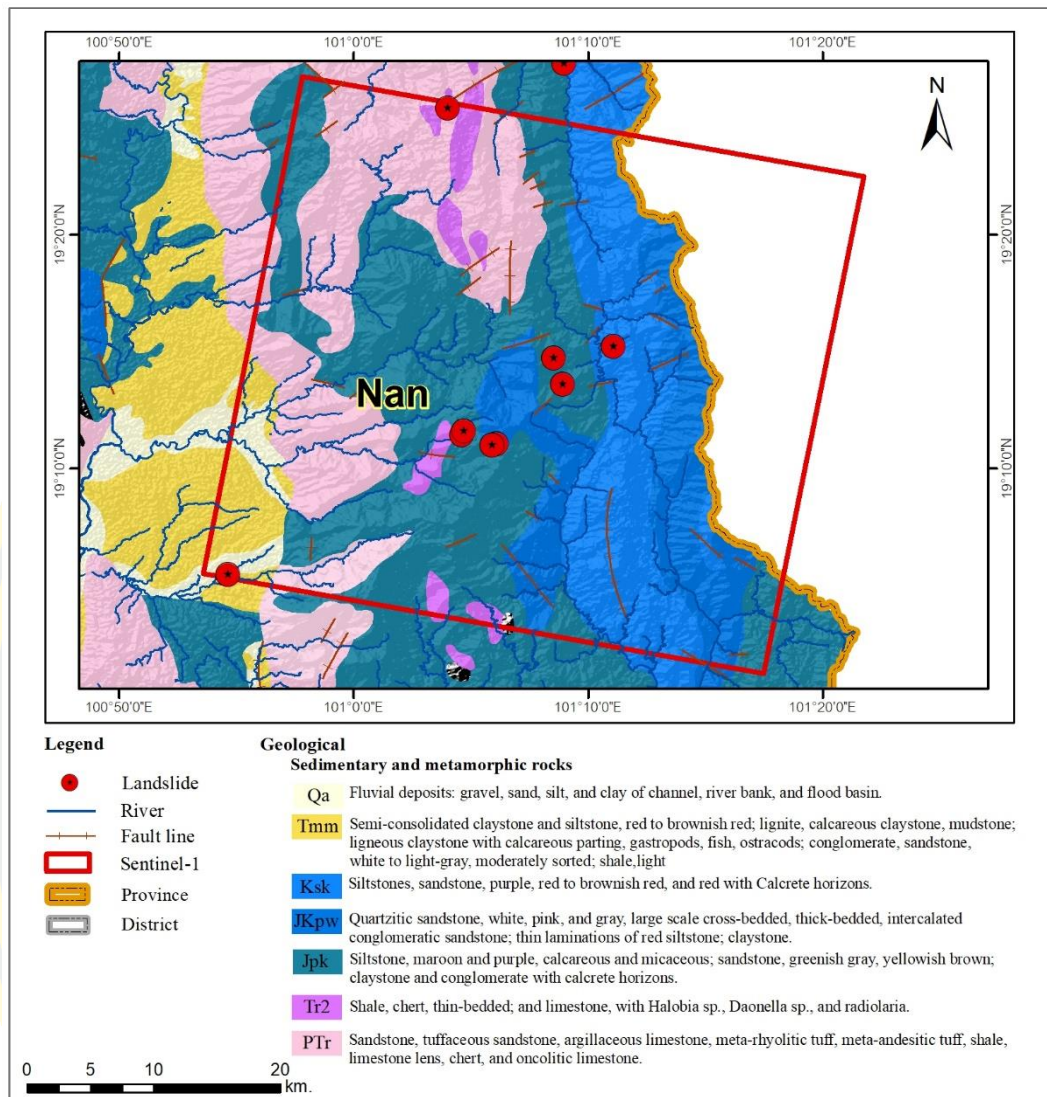


Figure 12: Geological structures of the study area in Nan, Thailand (Modified from Department of Mineral Resources)

3.2 Data

The SAR images, Sentinel-1A and 1B, were obtained from the European Space Agency with C-band in level-1 Single Look Complex (SCL) product containing phase and amplitude information. The polarization is vertical transmit and vertical receive (VV) with Terrain Observation by Progressive Scans (TOPS) acquisition mode and Interferometric Wide swath (IW). The ground resolution 5 meters are in range direction and 20 meters are in the azimuth direction. The acquisition time of data was taken from 2018 to 2019 and revisited time on six days. Sentinel-1 images in both

ascending and descending orbit were used to processing in this research. The information on Sentinel-1 data is shown in table 2:

Table 2: The information of Sentinel-1 data for PSI approaches

| PSI | Area | Orbit | Subswath | Year | Images | Total |
|-----|---------|------------|------------|--------------|--------|-------|
| PS | Beijing | Ascending | IW 2 and 3 | 2017 to 2019 | 62 | 130 |
| | Nan | Descending | IW 2 | 2018 to 2019 | 68 | |
| QPS | Beijing | Ascending | IW 2 and 3 | 2017 to 2019 | 62 | 139 |
| | Nan | Descending | IW 2 | 2018 to 2019 | 77 | |

Beijing case study in both city and rural areas that was spanning from May 20th 2017 to August 2nd 2019 with 80 total of SAR images. These images acquired in an ascending orbit. Subswath 3 was applied to city area that was used to PS processing, Subswath 2 was applied to the rural area that was used to both PS and QPS processing. Nan case study, 77 total of SAR images was spanning from June 26th, 2018 to October 1st, 2019. These images acquired in a descending orbit. Subswath 2 was used to both PS and QPS processing. The statistical information of the dataset in PS analysis is shown in figure 13 and 14 QPS processing is shown as figure 15 and 16.

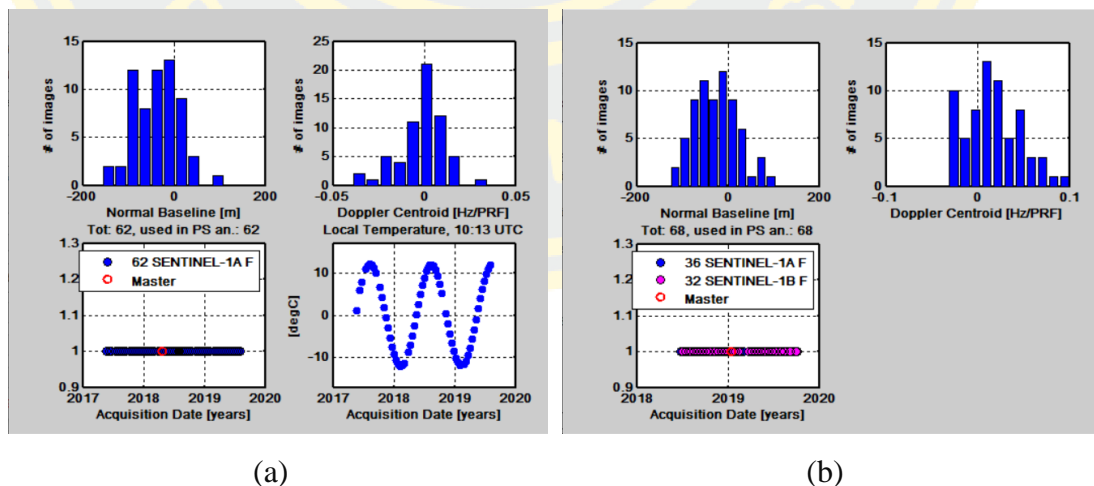
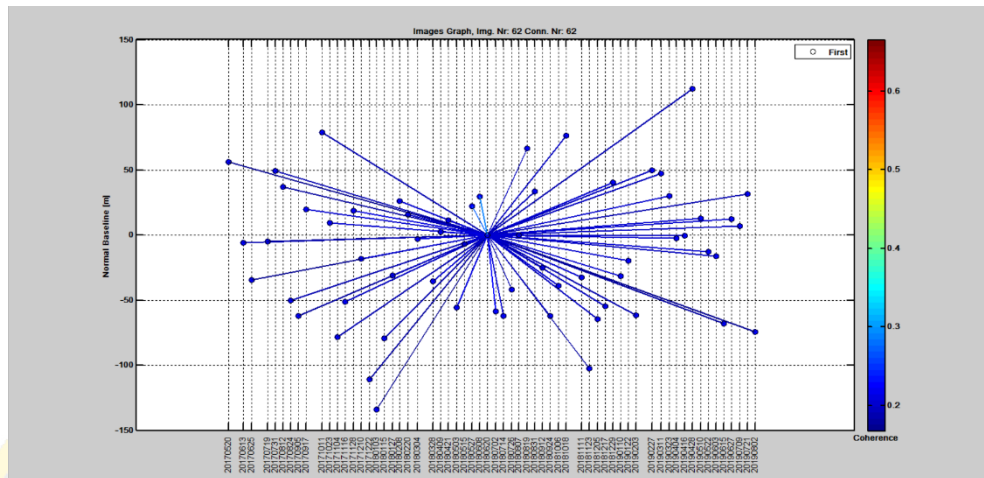
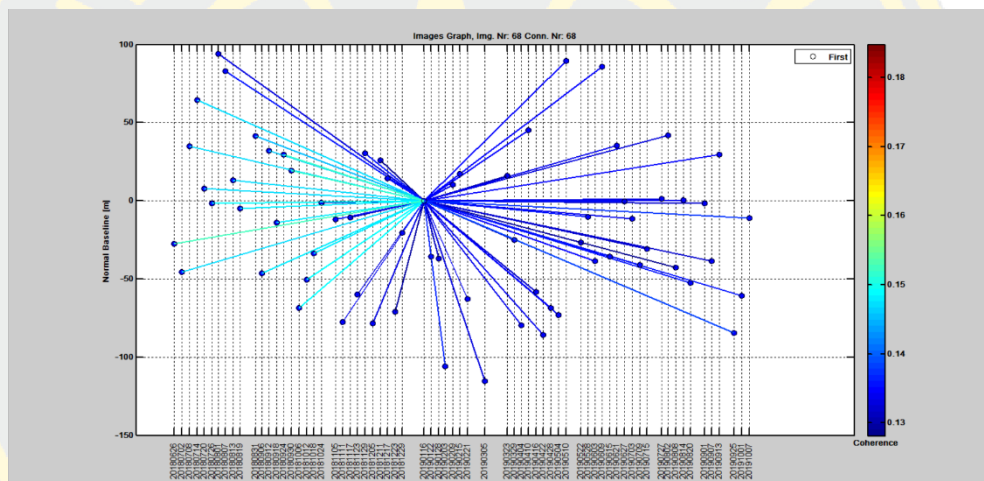


Figure 13: The statistical information of the dataset in PS analysis. (a) Beijing, (b) Nan.



(a)



(b)

Figure 14: The dataset of Sentinel-1 SAR images in the PS technique (a) PS technique in Beijing (city and rural) with 62 total number of SAR images. (b) PS technique in Nan with 68 total number of SAR images.

PS analysis, the Interferometric represented a star graph in the standard and temporal baseline, all images are connected as in figure 3-6, where each point presents an image in each connection an interferogram in Beijing and Nan. The time interval of the revisit is six days, and the longest interval is 12 days, which can perfectly assure the time correlation of the dataset. The normal baseline of the dataset is less than 150 meters. The short baseline can facilitate accurate registration and ensure good coherence to eliminate errors and atmospheric effects. The maximum Doppler center frequency is less than 0.05 Hz/PRF. The temperature variations about ten are ensuring stability for interferometry.

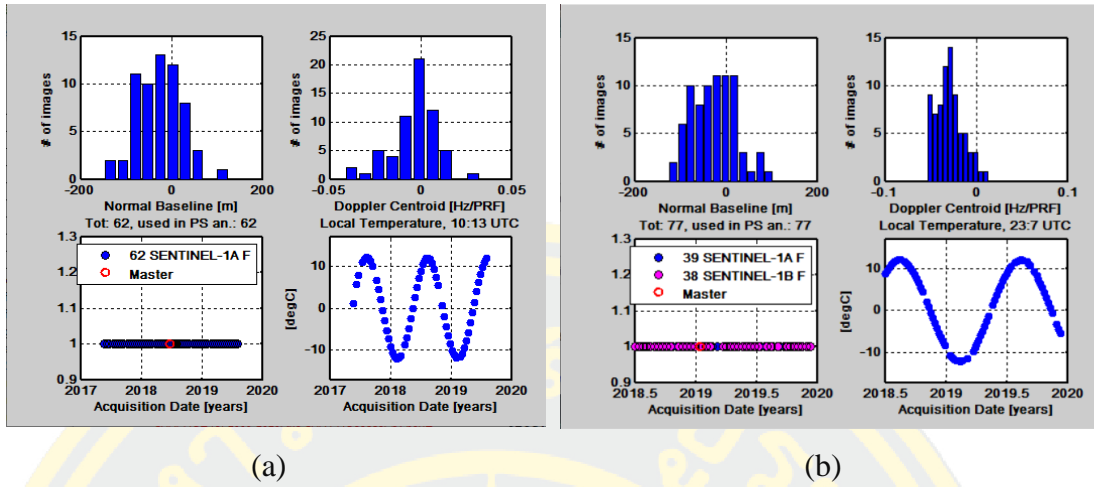


Figure 15: The statistical information of the dataset in QPS analysis. (a) Beijing, (b) Nan.

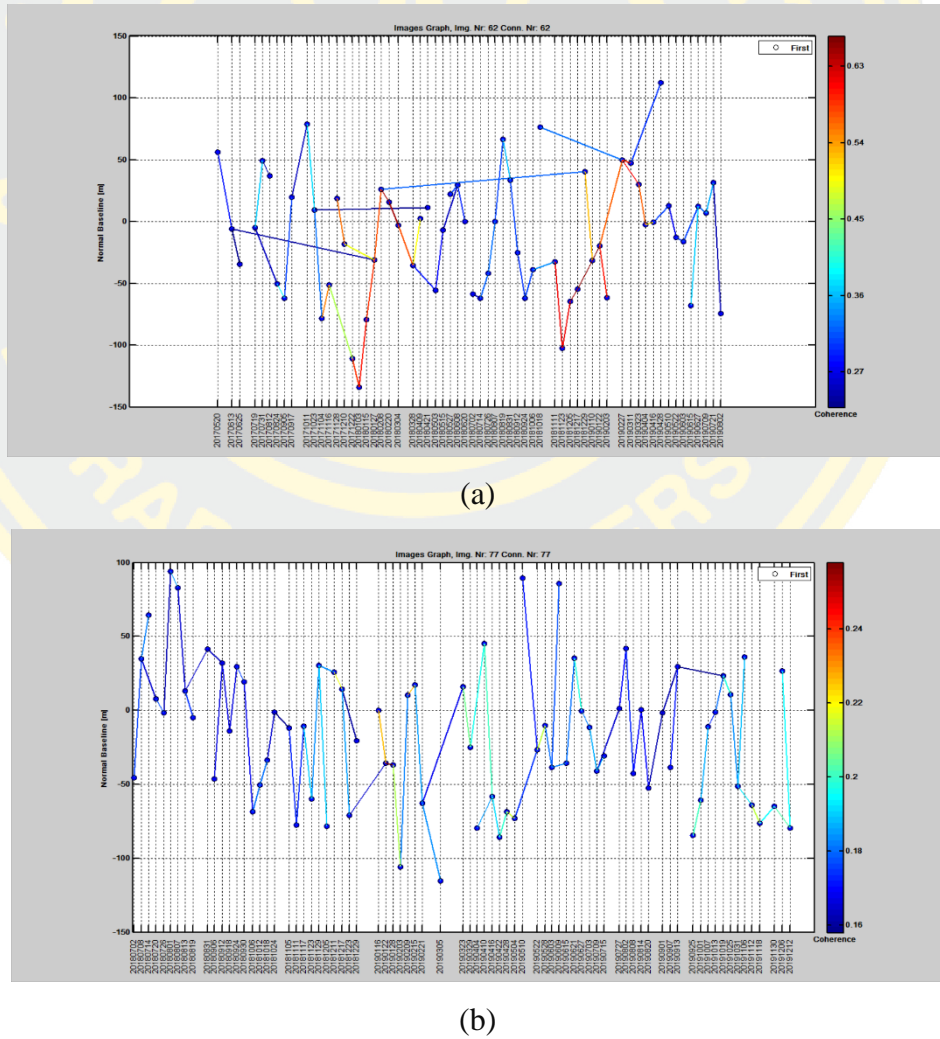


Figure 16: The dataset of Sentinel-1 SAR images in the QPS technique (a) The rural area of Beijing with 62 total number of SAR images. (b) Nan Province with 77 total number of SAR images.

QPS analysis, the time interval of the revisit is six days, and the longest interval is 18 days, which can perfectly assure the time correlation of the dataset. The normal baseline of the dataset is less than 100 meters. The short baseline can facilitate accurate registration and ensure good coherence to eliminate errors and atmospheric effects. The maximum Doppler center frequency is less than 0.05 Hz/PRF. The temperature variations about ten are ensuring stability for interferometry.

The graph connection assures the temporal continuity of the ground deformation measurements and thus the possibility of unwrapping. For the effective evaluation of an image graph (connectivity, number of links, and weight defined for difference graph), Minimum Spanning Tree (MST) image graph was applied to the rural of Beijing (a) and Nan (b). The selected areas are a vegetated area that has a high topology, and the number of PS is low.

3.3 Method

In purpose, to investigate and monitor ground deformation to increase the potential of identification, the landslide of the PSI technique in city and rural areas. This technique had a good accuracy on the surface deformation with the slow velocity, in which we used SARProZ software (refer to <https://www.sarproz.com/>) to processing the InSAR images and implement on Matlab software.

Persistent Scatterer Interferometry (PSI) is an advanced technique of Synthetic Aperture Radar (SAR) interferometry, which overcomes limitations of temporal and geometric decorrelation with repeat-pass satellite data (Greif & Vlcko, 2013). This research applies the PSI approach to investigate and monitor ground deformation. The trend of ground deformation is obtained by using InSAR time-series analysis of Persistent Scatterer: PS (A. Ferretti et al., 1999) and Quasi-Persistent Scatterer: QPS (Perissin & Wang, 2012) from Sentinel-1 images. The main of PSI processing are; generation of single master stack interferograms and removal of topographic phase, selection of PSC based on amplitude dispersion index, estimation and removal of atmospheric phase screen using PSC, and finding additional PS points (Alessandro Ferretti et al., 2001). PSI is the one important of principles time-series InSAR by analysis of phase difference using SAR images more than two images, which

shows the same position and a different time. As a result, the phase difference can analyze the deformation patterns that have various characteristics on the Earth's surface. Time-series images developed a multi-image approach in the images stack to measure the objects on the ground, providing consistent and stable radar reflections return to the satellite called Persistent Scatterer. This technique is suitable to identify the landslide, monitor the ground motions, and observe the triggering factor.

The interferometric phase signal, $\Delta\phi_{int}$, is the results of multiple contributions, that indicate the following terms (Massonnet & Feigl, 1998):

$$\Delta\phi_{int} = \Delta\phi_{topo} + \Delta\phi_{displ} + \Delta\phi_{atmo} + \Delta\phi_{noise} \quad (1)$$

Where $\Delta\phi_{topo}$ is the contribution of residual topographic height after the DEM subtraction from an interferograms. $\Delta\phi_{displ}$ is searched for displacement information. $\Delta\phi_{atmo}$ is the disturbance caused by Atmospheric Phase Screen (APS). $\Delta\phi_{noise}$ is the non-removable phase disturbance.

3.3.1 Persistent Scatterer (PS)

The PS technique is an advanced PSI approach to derive ground deformation with strong and stable reflectors, which use a single master image. The generation of interferograms is generated with respect to a single master and multiple slave images. The interferometric phase is generated by referring all images to a common master image to extract the information from a partially coherence target. The PS is used to explore stable point-like radar targets. This technique is based on the extraction of PS pixels, which mainly includes amplitude and phase deviation threshold method. The method works well in human-made structures, but it is difficult to be applied in heavily vegetated areas (Höser, 2018). The one limitation of the spatial density of PS point is coherent that it can provide hundreds of PS per square kilometers in urban areas and a few points in vegetated areas (Perissin & Wang, 2012). The PS technique is not suitable in the non-urban area because of less historical images in the mountain area and leading to the number of PS points, which are not enough to obtain accurate deformation results.

3.3.2 Quasi-Persistent Scatterer (QPS)

The QPS technique is an advanced PSI approach, which is able to extract information from the partially coherent target as the weight of phase estimation (M. Gao et al., 2019). Both spatial and temporal dimensions are different in QPS and PS. To clarify, the QPS is combined with both analysis of phase spatial and temporal correlation and used to analyze the complexity of the terrain. QPS technique is not only qualified in urban areas but also in vegetation areas that can improve the spatial density of QPS points (Razi, Sumantyo, Perissin, & Kuze, 2018). The Minimum Spanning Tree (MST) image graph configures the coherence as a weight in the estimation process was applied to maximum the coherent target. The limitation of spatial density detected of PS point has been improved significantly by QPS, allowing extracting the information from a partially coherent target. In particular, three main differences compared with classical PS approaches have been introduced. Firstly, in QPS, more than one reference image can be selected. Second, partially coherent targets of height and displacement that are only coherent weight for a subset of interferograms can be monitored. Third, spatial filtering can be applied to enhance the signal to noise ratio of the interferometric phase. The QPS technique is appropriate for an area where the density of permanent scatterer is not high (H. Chen et al., 2018), e.g., in the complex terrain changes and the low number of available images (Perissin, Wang, Prati, & Rocca, 2013b).

Therefore, the PSI processing provides a stable phase over the acquisition time span based on SARProZ software. PS-derived deformation velocity information by analysis of the backscattered signal from a network of individual, phase-coherent targets, co-registered, multi-temporal SAR images. Atmospheric Phase Screen (APS) estimation and Sparse Point processing are used to identify reflective ground deformation from phase component using Sentinel-1 time-series for a preferable understanding pattern of deformation with the cause of the landslide. In this research, PSI processing is divided into three sections: pre-processing, preliminary & geocoding, and InSAR processing is shown in figure 17.

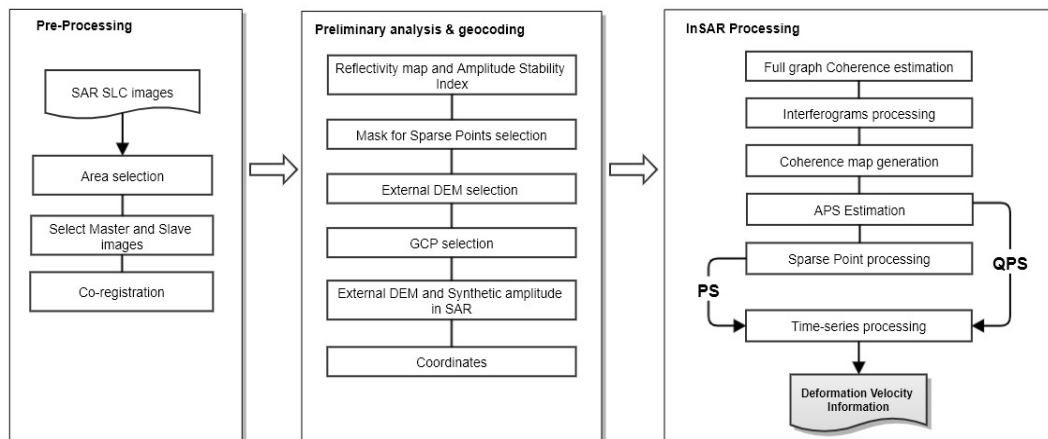


Figure 17: The conceptual framework for PSI processing

1. Pre-processing

In the first section, pre-processing is an area selection to determine the interesting site to single interferometric pair, which was used Sentinel-1 ascending and descending orbit. Firstly, the selection of master and slave before the co-registration process. The optimal master image selection considers to geometric and period time of the normal baseline and temporal baseline, slave images are co-registration to master image for the single master stack. The images are taken from a slightly different time. It is necessary to co-registration for the combined phase of two SAR images by precise orbit. The correlation window is used to search for offsets between master and slave images, which can reduce geometric error. The co-registration is essential for the accurate determination of phase difference and noise reduction.

2. Preliminary and geocoding

The second section, preliminary and geocoding is generated reflectivity map as the temporal average and temporal standard deviation of all images, which select the pixel closest to the target position by the local maximum of the incoherent time average of the image amplitude. The external DEM was selected Shuttle Radar Topography Mission (SRTM) 1 arcsec resolution (30 m. x 30 m.) for topographic phase removal, the height generated from external DEM (SRTM). Ground Control Point (GCP) was selected to geocode; the selected point must be chosen within unaffected areas by ground motions to avoid the retrieval of an unreal pattern of deformation. The

coordinate algorithm is a projection of SAR data in geographic coordinates, which uses an external DEM to account for geometric distortions.

3. InSAR processing

In the third section, InSAR processing is an implementation of InSAR data to conduct the deformation velocity. The Interferogram referred to master and slave images allows accurate measurements of the displacements of radar targets along the satellite line of sight (LOS) by computing the difference of the phase values two SAR images gathered at different times the whole same area of interest. The coherence estimation referred to the amplitude of the correlation coefficient between two SAR images, such as decorrelation due to the temporal and geometric degradation and elevation of the image pixels after flattening and DEM removal, which presents information of phase quality, noise, etc. Atmospheric Phase Screen (APS) estimation can estimate with Persistent Scatterer by estimating and removing the geometrical and movement components; it is possible to reach the delay induced in the atmosphere. For the selection of Persistent Scatterer candidates (PSC) obtained with Amplitude Stability Index to analyzing neighbor target that has a probability to highly coherence. The temporal phase series associated with each connection of PSC measurement for the relative height and deformation trend. An integrated the small atmospheric contributions through the spatial graph and relates to the spatial unwrapping of phase residuals. It is solved noise due to the high over-determination obtain by the redundancy of connections graph. Grid phase unwrapping is a sparse estimate and removes the atmospheric phase delay, orbital, and DEM residual error for each Interferogram. Sparse Point processing was selected over the Amplitude Stability Index with a threshold lower than for APS estimation to increase the number of detected points. Both thresholds in APS and Sparse Point processing determined in the previous step were applied to measurement displacement values for each point. The high temporal coherence index greater than 0.7 were selected for analysis to ensure high coherence and stability.

Lastly, the Displacement time-series module was derived from the deformation velocity rate in each point precise with millimeter/year along the Line of Sight (LOS) from a subset of the filtered coherent Interferogram. All the detected points

related outputs such as velocity, displacement time series, cumulative displacement, height, height relative to the ground, temporal coherence, and KML files. The results were identified by evaluating the dispersion of phase residuals through the temporal coherence. Google earth is a basic software to interprets velocity points and estimate susceptibility areas.



CHAPTER IV

RESULTS

This chapter provides the result of the PSI technique, which observed in Beijing and Nan. The result is the displacement taking place between two acquisitions, which represents a precise technique to increase the ground deformation measurement in the radar line of sight direction (LOS). The deformation trend provides more accurate delineation for susceptibility areas to landslide monitoring.

4.1 Ground deformation velocity map from PSI processing

The PSI results are present the ground deformation velocity rate in the LOS direction of the satellite. The result was expected to be detected PS and QPS points whole the study area with a high temporal coherence threshold of 0.7 for the high quality of phase difference. Thus, it is appreciable the density of points, even in the vegetated areas and height details, that can be easily recognized (Perissin & Wang, 2012). Also, it can be observed that most of the topographic in reflectance of the slope. However, this research was no access to the ground truth; the reference point was selected in an area that there assumes a stable area. The deformation trend can be estimated for the susceptibility area and landslide by visual interpretation. For visual interpretation; The motion negative away from the sensor and the motion positive toward the sensor, with value was ranging mm/yr. The temporal coherence threshold between 0.7 to 1.0 is highly significant at each point.

4.1.1 Persistent Scatterer (PS)

1. 1 Beijing case study

In PS analysis, the displacement map shows the ground deformation velocity rate of Beijing case study in both city and rural areas. The displacement velocity map of this area with scattered distribution point target was generated with Sentinel-1 SAR images acquired from 2017 to 2019, a total of 62 images. The motion negative away from the sensor (red) and the motion positive toward the sensor (blue).

The city of Beijing, China, PS candidates were selected threshold of 0.75 for the Amplitude Stability Index. The PS points found that 378,995 points (approximately

227 points/square kilometer). The high density of PS candidates and good temporal coherence ensures the solution for time-series processing that the averages displacement map can finally be derived as figure 18. The displacement rate range from -99 to 19 millimeter/year was identified by PS analysis. This area provides the quantitative result of ground deformation in Beijing city. Thus, the PS points are mostly observed in human-made targets, and they are aggregated in residential areas.

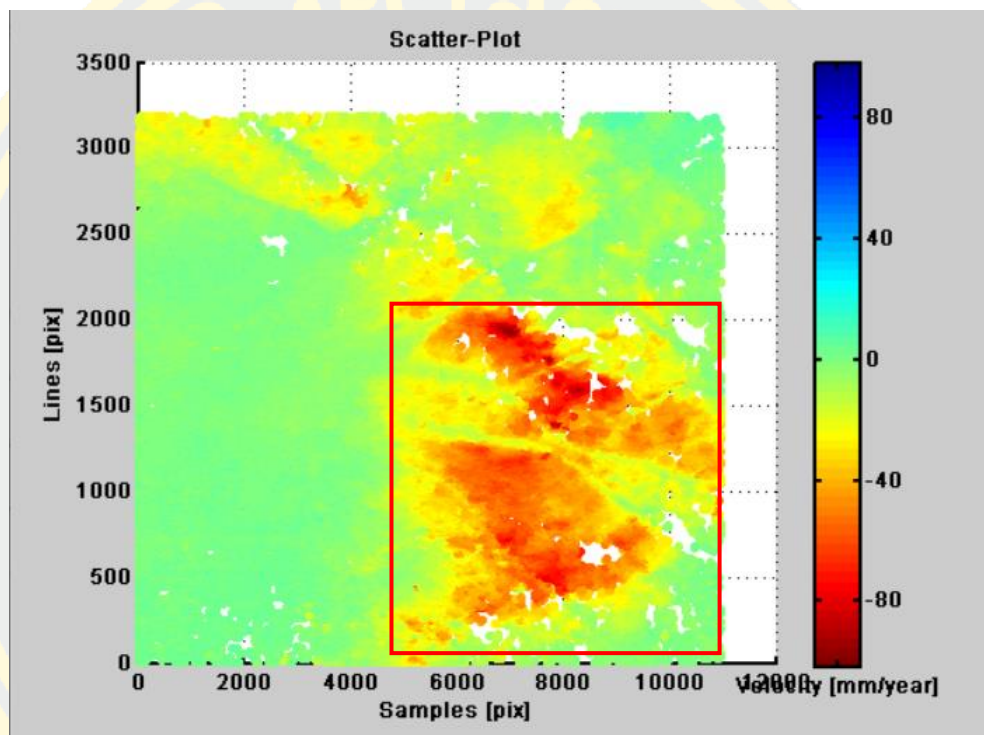


Figure 18: The ground deformation velocity map in Beijing city case study with PS analysis, The color bar range of -100 to 100 mm/yr.

The plain area in the eastern part observed a serious displacement (red) in Chaoyang, Tongzhu, shown as figure 19. These areas are economic zones, an industrial area. The most susceptibility area over to 99 mm/yr in Chaoyang and Tongzhu district shown as figure 20. The displacement is consistent with the groundwater overexploitation, water withdrawal for industry, and people's daily lives, another important factor causing underwater level change may be related to construction dewatering. The center of the city appears stable (green) to slightly area (yellow). The susceptible areas related to the geological structure, the density of buildings, the distribution of infrastructure.

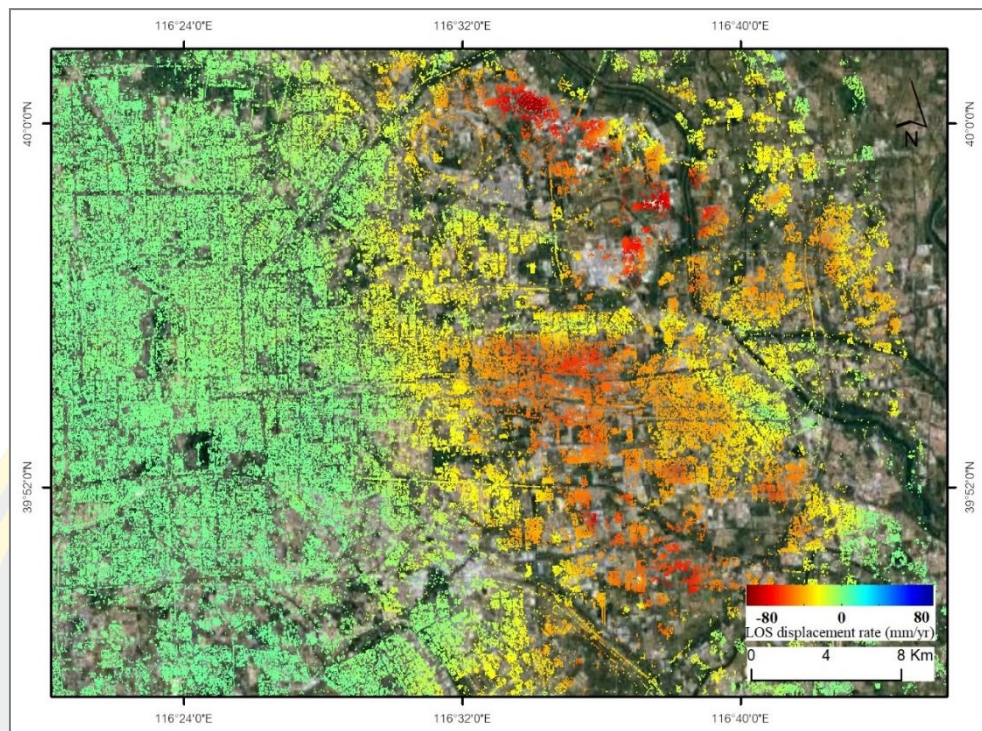


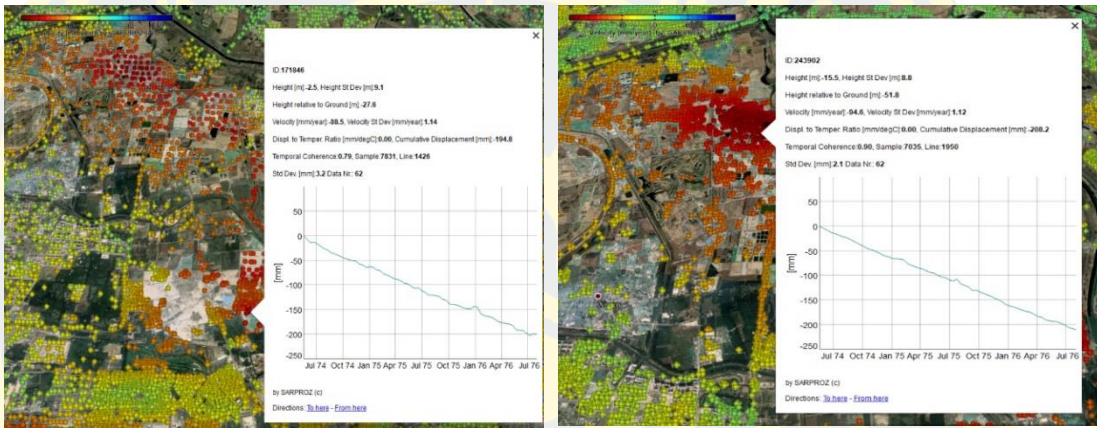
Figure 19: The serious displacement centers are observed in Chaoyang and Tongzhu district, overlay on Google Earth.

Beijing city is in flat topography, in which the main component of Quaternary sediment is clay, intervened by sand with groundwater condition. Moreover, it is greatly affected by rainfall and surface water; also, human activities are triggering factors for land subsidence, particularly overexploitation of groundwater are used to an industrial and residential area. Also, soft soil consolidation is in most areas, which can cause subsidence when underground water is withdrawn. In addition, the other factor such as geomorphological fail and lithological characteristics have an impact to the subsidence rate.

Mostly of ground extraction has been occur in the suburban area. The displacement was assumed to be mainly vertical as subsidence. The PS processing can provide high PS density that it is possible to exploit PS candidates for the construction, e.g., building, road, and railway. It is interesting to note that this area is across affected by deformation rates.



(a)



(b)

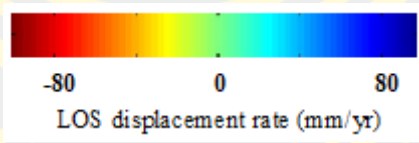


Figure 20: The displacement patterns using the PS analysis

The rural of Beijing, China, PS candidates were selected a threshold of 0.65 for the Amplitude Stability Index. The PS points found that 43,981 points (approximately 26 points/square kilometer). The displacement rate range from -42 to 27.75 millimeter/year was identified by PS analysis shown as figure 21. The high displacement rates were observed in the Mentougou district. Mostly of PS points were identified in human-made structures, e.g., road and building. The mountainous were observed mostly stable areas in the central part and slightly displacement of 7.0 mm/yr in southern (green) and north-east (yellow). Whereas that some areas unable detected PS points due to the lack of urban areas and the densely vegetated areas shown in figure 22.

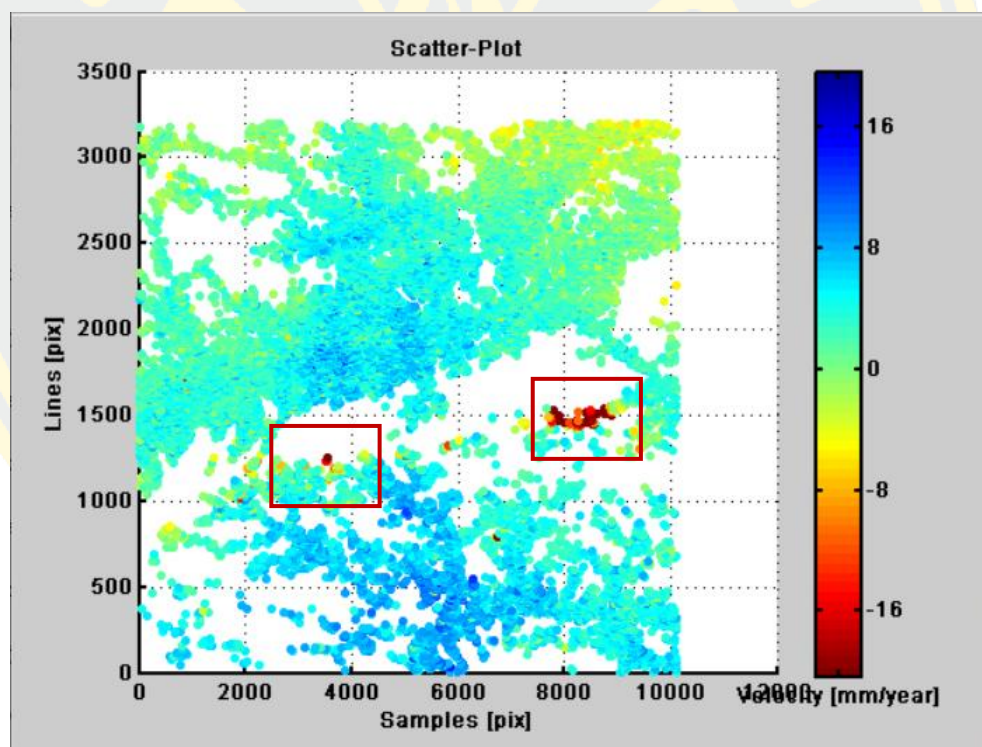


Figure 21: The ground deformation velocity map in Beijing rural case study with PS analysis, The color bar range of -20 to 20 mm/yr.

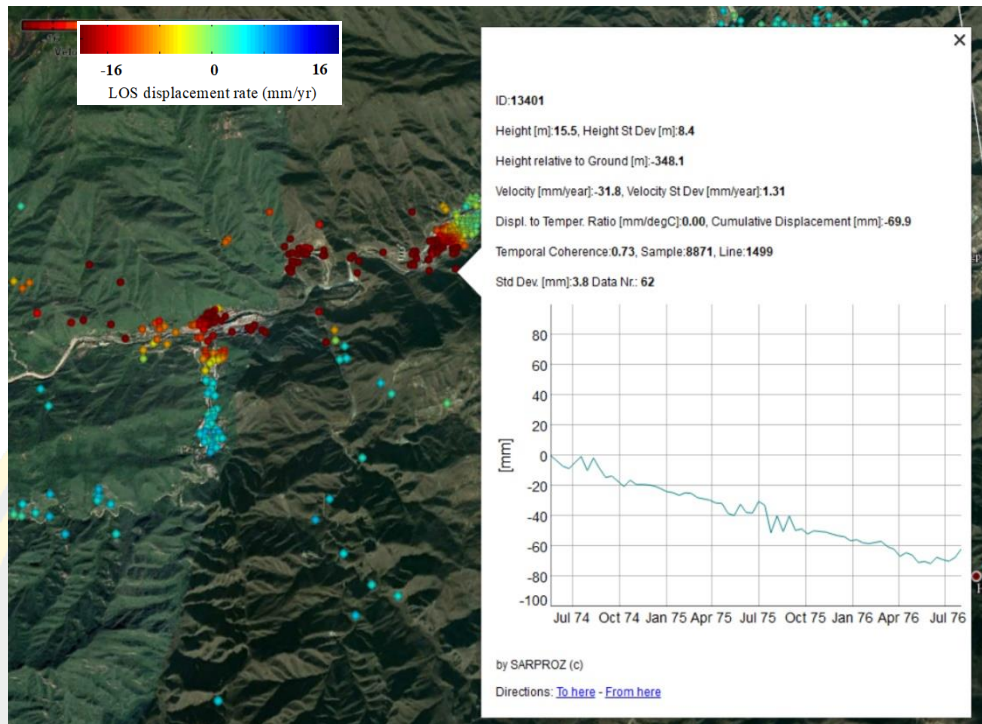


Figure 22: The serious displacement centers are observed along the road and building in the Mentougou district.

1. 2 Nan case study

In PS analysis, the displacement map shows the ground deformation velocity rate of Nan case study in Thailand. The displacement velocity with scattered distribution of point target was generated with Sentinel-1 SAR images acquired from 2018 to 2019, a total of 68 images.

The results in the Nan case study in Thailand, PS candidates were selected threshold of 0.65 for the Amplitude Stability Index. Although, the PS points found that 1,966 points, the highly temporal coherence of 0.7 that found only 118 PS points. The displacement rate range from -22.75 to 17.5 millimeter/year was identified by PS analysis shown as figure 23.

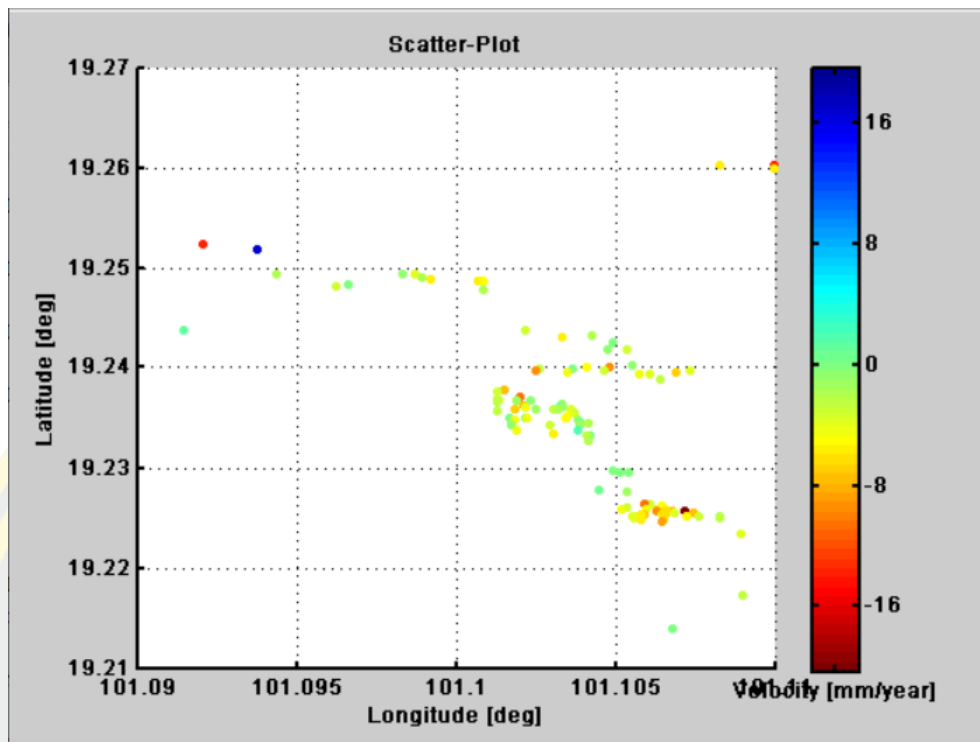


Figure 23: The ground deformation velocity map in Nan case study with PS analysis, the color bar range of -20 to 20 mm/yr

Nan area is a sedimentary and metamorphic rock, also is located in the tropical zone. The main agricultural is cash crops in the highland as rice farming, maize, forest products. Thus, PS is affected by temporal changes due to vegetation and unable identified by subjecting the amplitude of the pixels in all available data. The displacement rate is low precise even in vegetated and forested areas. Moreover, the landslide was unable to investigate due to promising conditions concerning steep slope, land cover, slope angle, strong vegetation areas. Therefore, the PS analysis obtained a few points along the roads and villages because of the object target is moving with the vegetation and terrain shown as figure 24.

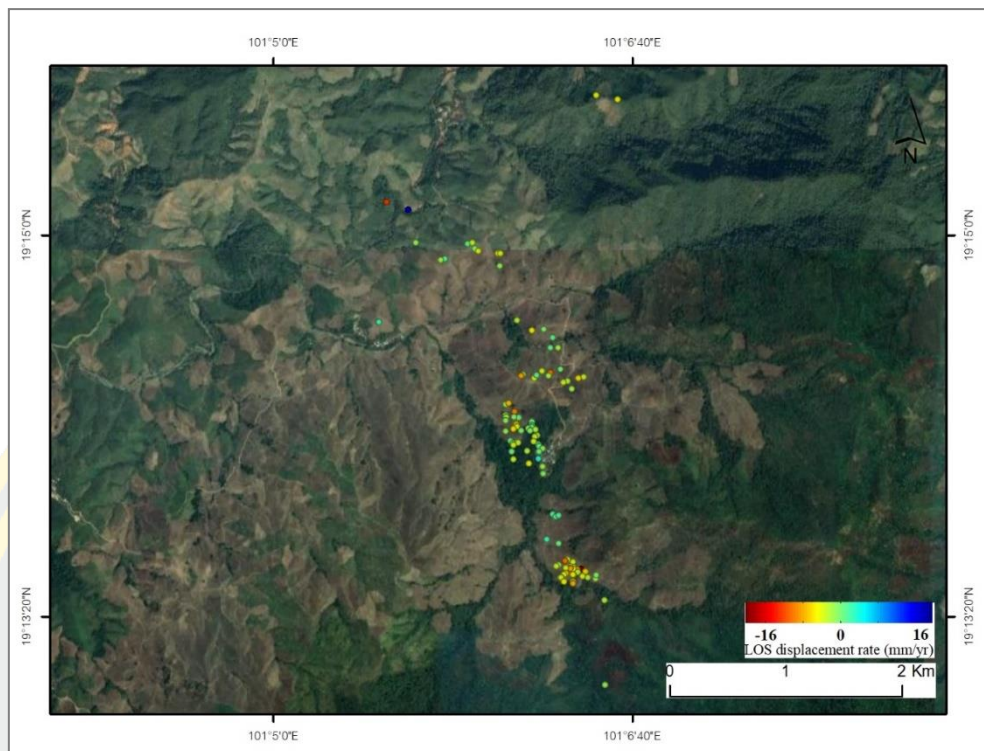


Figure 24: The displacement map of PS analysis along LOS direction, overlay on Google Earth in the Nan, Thailand.

The PS result in Beijing was efficiently detected where the ground covering with man-made objects, but PS results in Nan was inefficiently detected that show as the number of measurement points and also pattern of the displacement was not clear to use to analysis. Thus, the detected of 118 points were observed in Nan, while PS of 43,981 points and 378,995 points were observed in Beijing (coherence of 0.7).

4.1.2 Quasi-Persistent Scatterer (QPS)

2. 1 Beijing case study

In QPS analysis, the displacement map shows the ground deformation velocity rate of the Beijing case study in rural areas. The displacement velocity map of this area with scattered distribution of point target was generated with Sentinel-1 SAR images acquired from 2017 to 2019, a total of 80 images.

In the rural of Beijing, China, PS candidates were selected a threshold of 0.6 for the Amplitude Stability Index. The QPS points found that 107,266 points

(approximately 62 points/square kilometer). The displacement rate range from -68 to 142 millimeter/year was identified by QPS analysis shown as figure 25. The QPS results were dissimilar results of PS. Meanwhile, the spatial distribution of QPS points is homogeneous both in urban and non-urban areas. Besides, one displacement was detected in eastern, which provides similar to PS analysis. This technique with obvious motion was detected from QPS analysis.

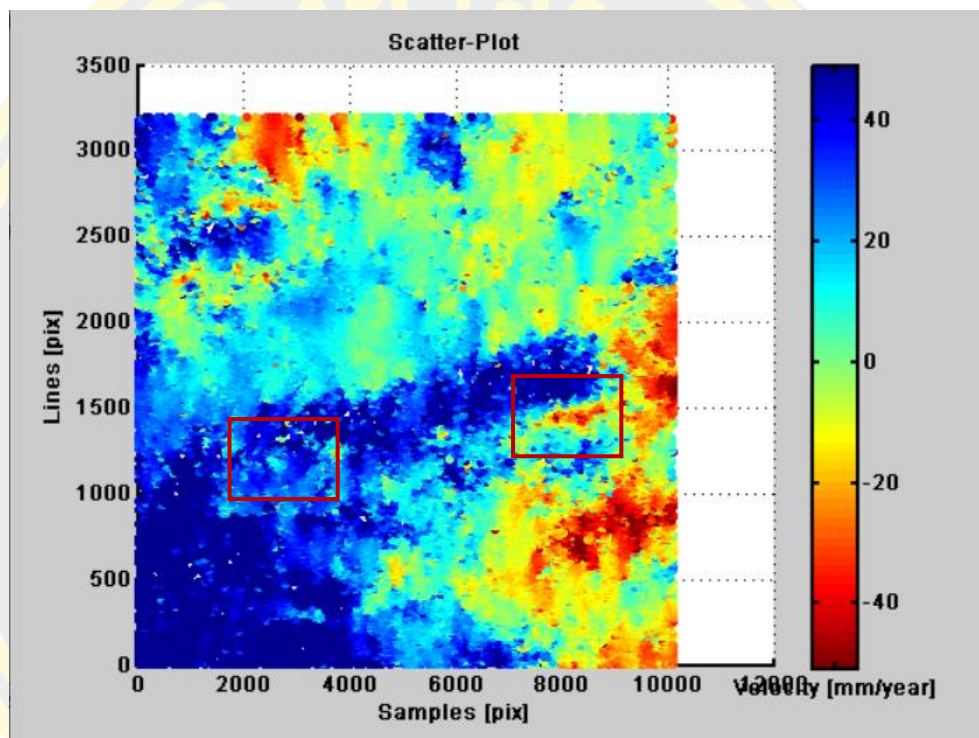
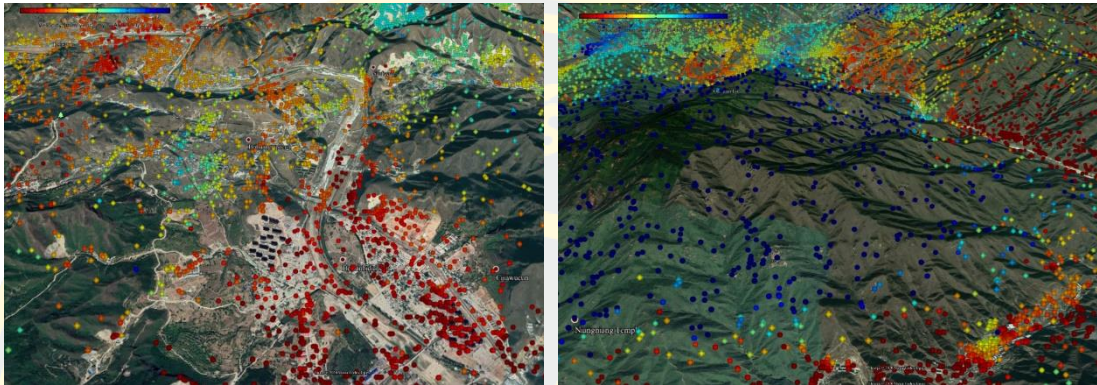


Figure 25: The ground deformation velocity map in Beijing rural case study with PS analysis, the color bar range of -50 to 50 mm/yr.

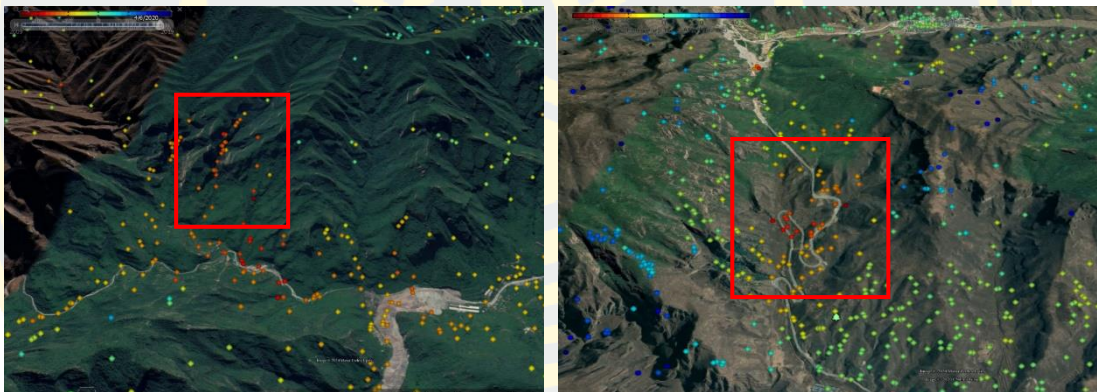
The QPS was performed a better than the PS, that it indicates to analyze the pattern and susceptibility area. However, some differences were obtained, mainly concerning the density and location. Due to an ongoing of the structure, the linear trend of negative velocities (red) all over the area is reasonable, where the structure area has been moving far away from the sensor, relative to LOS direction. In contrast, the linear trend of positive velocities (blue) without any man-made structure is moving toward the sensor show as figure 26.

The highest velocity in the mountain on the southwest was observed a serious displacement (blue) with rates over to 142 mm/yr, which there is a distinct pattern of

increasing velocity towards the top slope of the hill. The land movement is the highest failure that can occur landslide in the future. Because of this area is mostly a natural terrain also lack of man-made structure, while urban was detected in several displacement areas, especially along the road and the building.



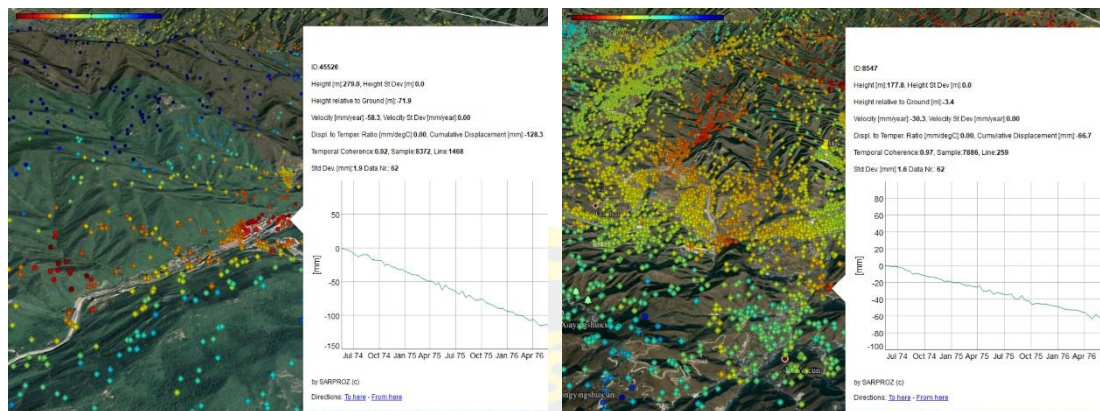
(a)



(b)



(c)



(d)

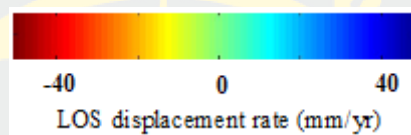


Figure 26: The displacement patterns using the QPS analysis. The color bar ranges from -50 to 50 mm/yr.

2.2 Nan case study

In QPS analysis, the displacement map shows the ground deformation velocity rate of Nan case study in rural areas. The displacement velocity map of this area with scattered distribution of point target was generated with Sentinel-1 SAR images acquired from 2018 to 2019, a total of 77 images.

The Nan case study in Thailand, PS candidates were selected a threshold of 0.55 for the Amplitude Stability Index. The PS points found that 55,738 points (approximately 32 points/square kilometer). The displacement rate range from -262 to 248 millimeter/year was identified by QPS analysis shown as figure 27. The motion negative away from the sensor (red) and the motion positive toward the sensor (blue). Despite dissimilar between the results obtained by both PS and QPS approaches, significant differences in density point and distribution point was detected. However, the several displacements were performed to assess the instable area, that focuses on high-velocity rates shown as figure 28.

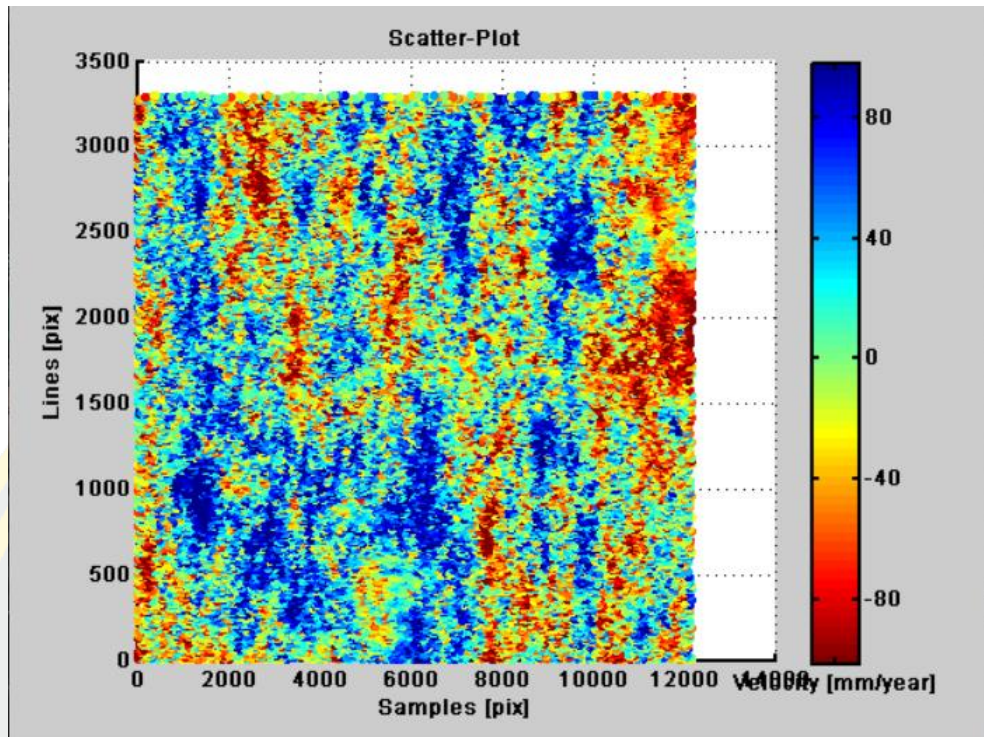


Figure 27: The ground deformation velocity map in Nan case study by QPS analysis, color bar range of -100 to 100 mm/yr.

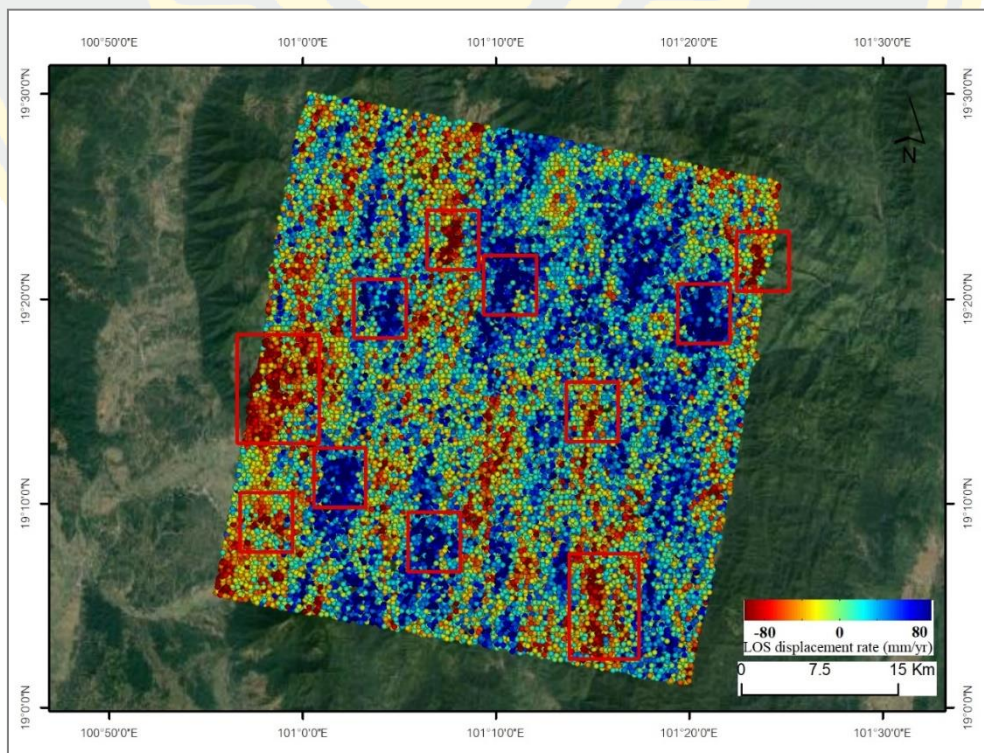
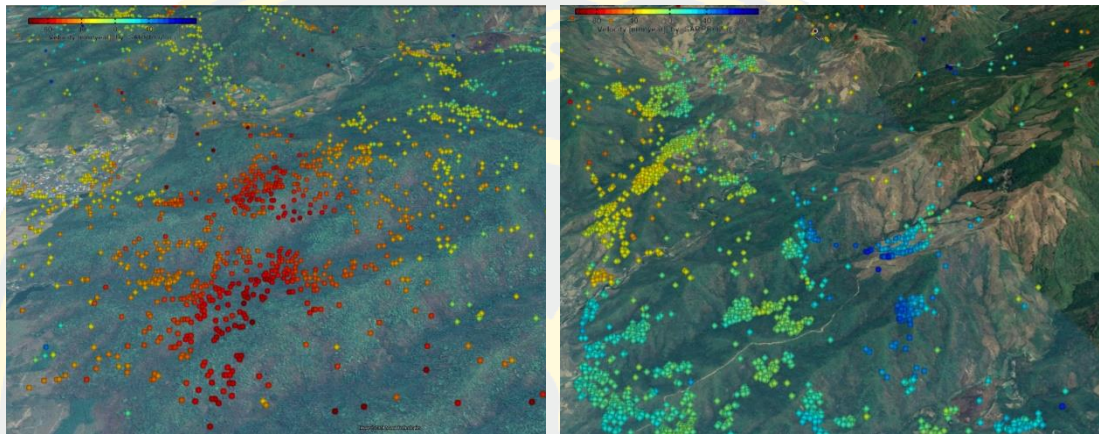
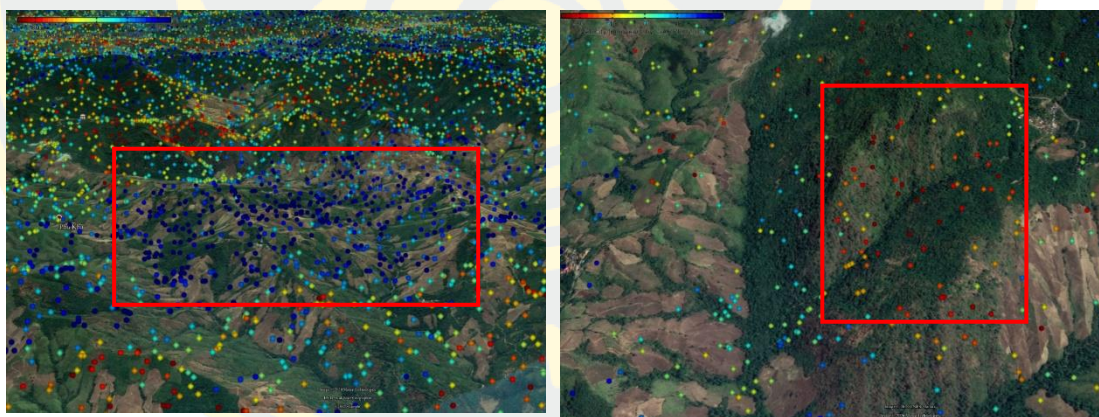


Figure 28: The displacement map focus on high-velocity rates, overlay on Google Earth.

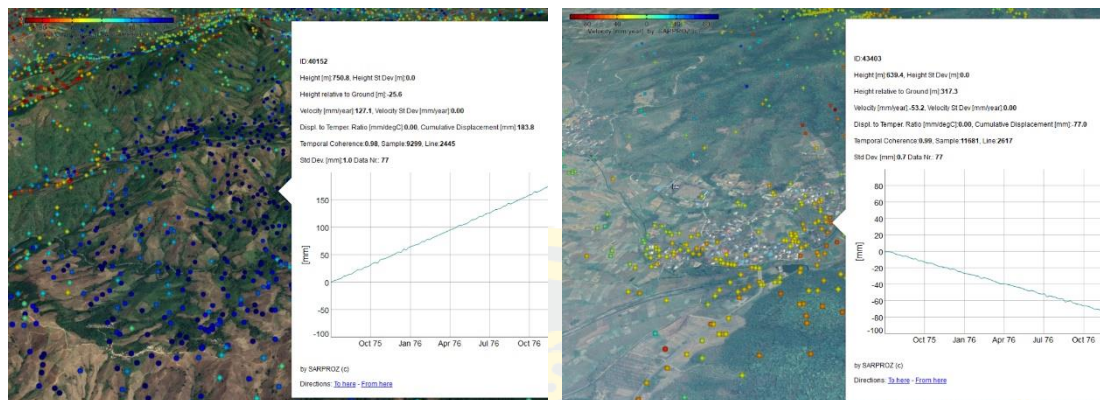
The result shows that the distribution of QPS points is not clear to identify the landslide. The QPS approach produces a denser point that is higher than the PS approach. The highest displacement appears in agricultural and forest (blue, red), with velocity rates of -268 mm/yr shown as figure 29.



(a)



(b)



(c)

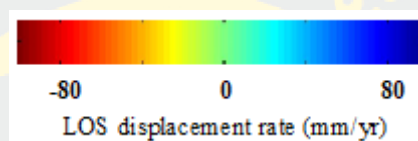


Figure 29: The displacement patterns using the QPS analysis. The color bar ranges from -100 to 100 mm/yr.

The topography in Nan are steep slopes and deep valleys that have a potential influence on erosion and heavy runoff. Also, the continuity of heavy rainfall on slope failure is exposed to severe landslide, especially along the river and the hill where the cut of a slope.

The QPS was efficiently applied to vegetation areas and improved the number of measured points that were detected points more than the PS points. The detected of 107,266 points in Beijing, and 55,738 points in Nan were observed (coherence of 0.7). However, the results have difficultly analyzed and interpreted the pattern motions because a lot of noise that was not eliminated.

4.2 Landslide identification

The ground deformation was obtained from both PS and QPS, which defined as the susceptibility areas. The landslide can be observed where the cumulative of detected points having the dominant value. The result in Beijing rural was identified landslide in Fangshan district but results in Nan was unable identified any occurred landslide.

The Beijing study area has been successfully detected the landslide from both PS and QPS. The map shows displacement where a landslide was confirmed to occurred near Mixi road in Fangshan district with PS analysis shown as figure 30. The displacement occurs in the rates of a slow-moving landslide, the motion of 5 mm/yr.

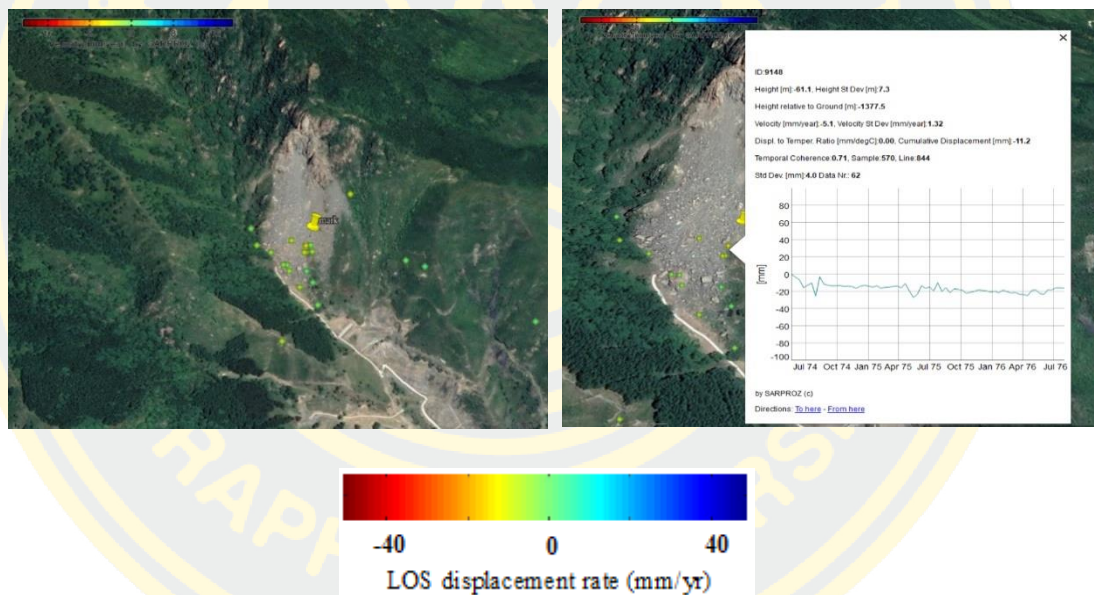


Figure 30: The one landslide has been detected, located near Mixi road in Fangshan district.

The two landslides were detected by the QPS analysis, shown as figure 31. The density of QPS within the area where the occurrences landslide is relatively low. Therefore, there is no clear visual difference between the velocity rates inside the potential landslide area, as was observed in the Beijing case study.

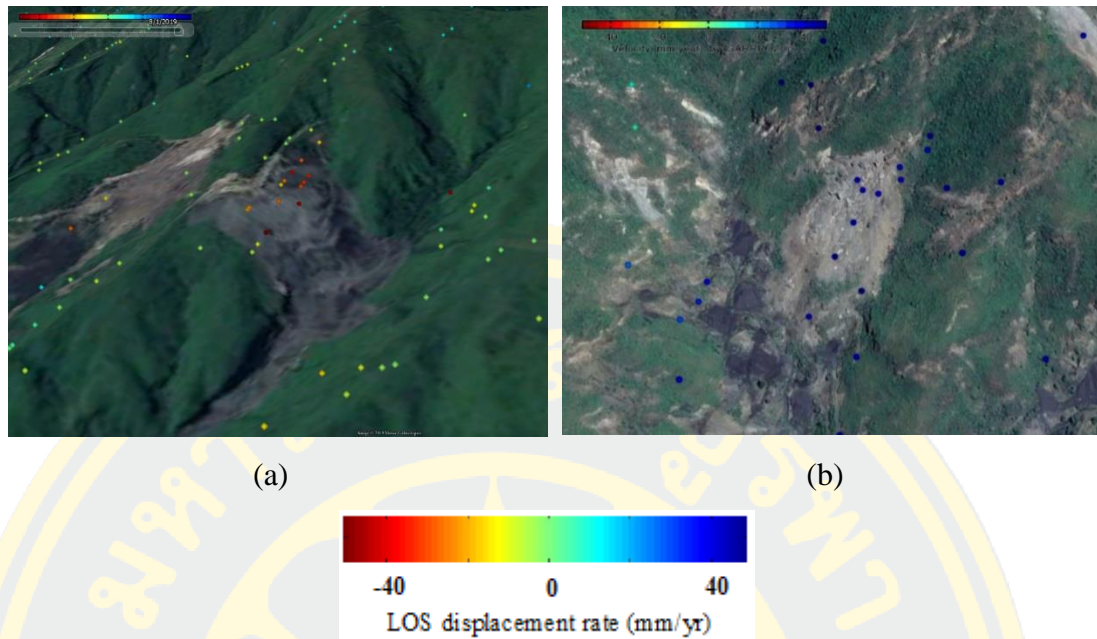


Figure 31: The two landslides have been detected. These landslides located in Fangshan district (a) and (b) Yuta road

The landslide types are controlled by the weathering pattern and by the morphology of slope. Type of landslide seems as debris flow and translational slides, triggered along steep slopes. These occur mainly failure material of soil and highly weathered rocks.

The landslide in Nan case study was unable to investigate QPS analysis, similar to the PS analysis. Due to promising conditions concerning the steep slope, the cover of the forest whole the study area, the vast area of agriculture, there always moving. Thus, PSI was unable to analyze this complex area better an area with a permanent structure. The displacement value obtained from this technique probably sufficient for the analysis of unstable in this area that the highest failure can occur landslide in the future. However, the QPS can be provided QPS points all over areas; the trend of deformation was not identified as the landslide location. Because of the results are filled with noise, making the displacement map not accurate, which is unreliable and difficult to interpret the pattern of motion. Also, the result contains possible ground displacement along with noise, which can be eliminated if the coherence between two SAR images is high.

4.3 Connection graph of PS and QPS processing

The comparison of PS and QPS approach, shows the different connection graph between two approaches; the connection graph of temporal coherence, the temporal coherence estimation, and the scatter plot of deformation velocity rate that obtained the threshold of 0.7 temporal coherence.

4.3.1 Temporal coherence estimation

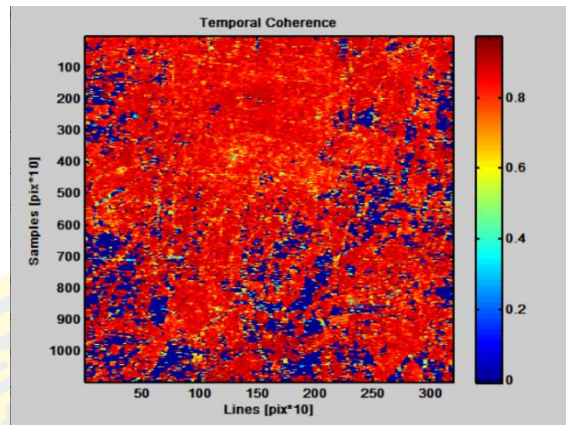
The coherence is the connection of interferogram. It can be used as a quality map where the pixels with higher coherence indicate high-quality observations. Coherence refers to the accuracy of the result; if less coherence, there have some noise and low accuracy. The maximum coherence value measures from the reference point and follows the highest coherence available in the neighborhood of already solved pixels. The reference point was selected in a stable area.

The coherence map represents the signal to noise ratio, with white being 1 meaning full signal strength and black being 0 meaning no backscattering. Temporal coherence of PS in Beijing city has high coherence, and another two cases study has constant on the slope of the mountain, which has the low to nonexistent coherence. The coherence of QPS in Beijing rural has better than the Nan case study has poor coherence due to the satellite direction and the connection of the reference point of all images. Thus, the coherence map of the target region suggests that more than a threshold of 0.7 coherence is better.

High coherence presents the high quality of phase difference (red), and low coherence presents low quality (blue), that is highly noise of phase difference. In addition to this value is an influence to connect the processing of the Sparse Point.

1.1 Temporal coherence of PS processing

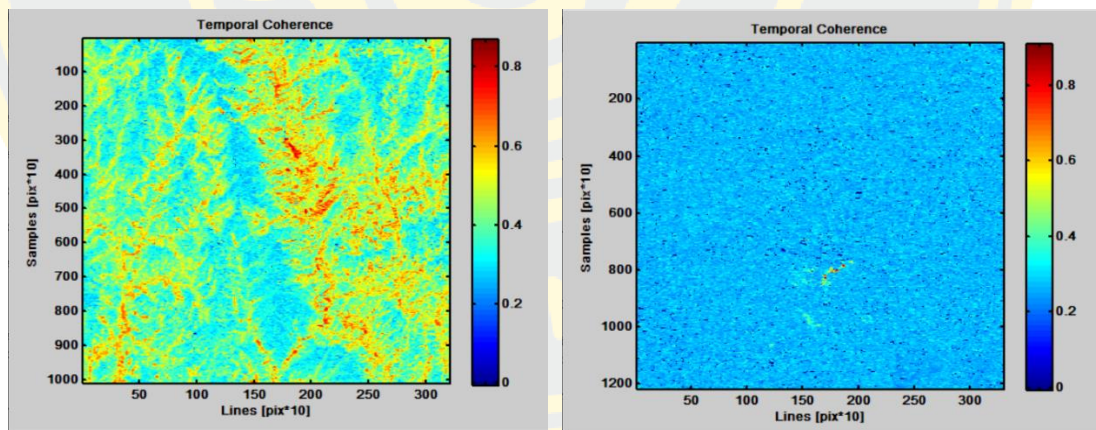
The temporal coherence graph in the Beijing city is high performed (red), resulting from the efficiency of connecting an interferogram. Most of the coherence more than 0.7 are observed in urban, but a non-backscatter point on miscellaneous and another area (blue) shown as figure 32.



(a)

Figure 32: The temporal coherence estimation in Beijing city case study with PS analysis

The temporal coherence graph in the Beijing rural is moderately performed, resulting in low land (red), poor resulting in the top of the mountain (blue, green). Apart from the temporal coherence graph in the Nan is performed low in very poor phase maps, the highest value, where pixel close to the reference point shown as figure 33.



(a)

(b)

Figure 33: The temporal coherence estimation of PS processing. (a) Beijing rural, (b) Nan case study

1.2 Temporal coherence of QPS processing

The QPS has not been improved the coherence in Nan shown as figure 34. The coherence graph is very poor (blue). Temporal coherence is high in low land (red). As a result of the steep topography, geometry, and densely vegetation limits the coherence between successive SAR acquisitions, that effects of limitation perform to individual the trend of deformation.

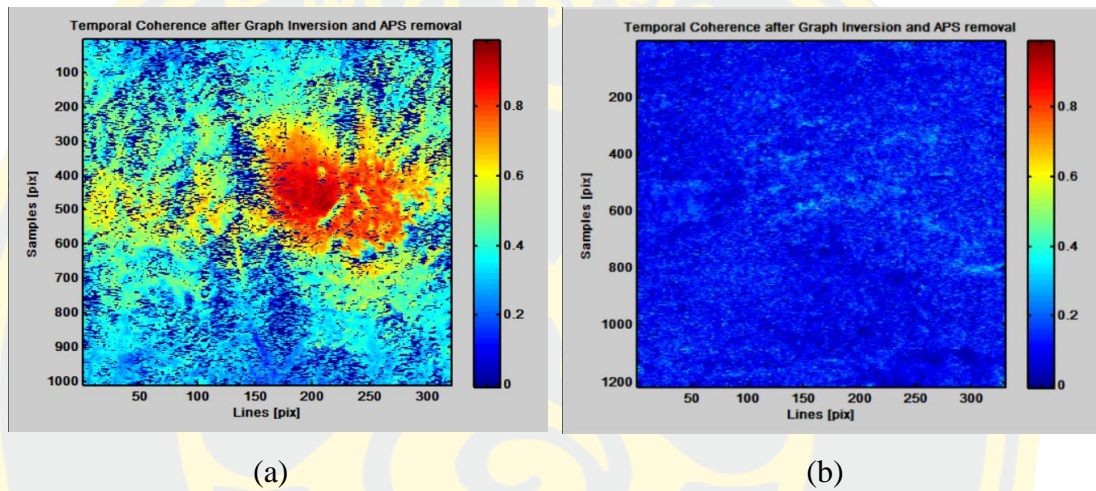


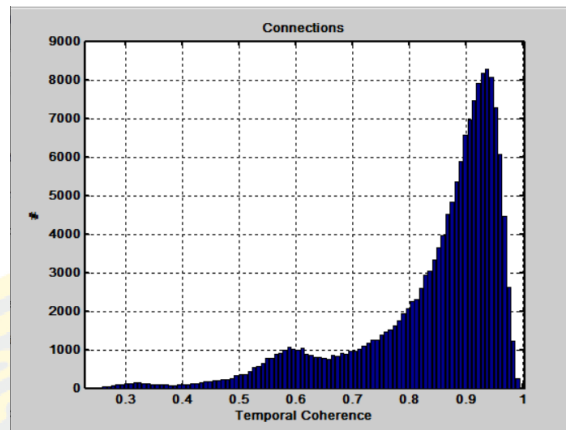
Figure 34: The temporal coherence estimation of QPS processing. (a) Beijing rural, (b) Nan case study

4.3.2 Connection graph of temporal coherence

The distribution of temporal coherence can give more detail to explain the different results. The temporal coherence can be recognized as the average closeness of the phase, with consideration to the reference point. The graph could be a trend to 1, and more coherence is better analyzed.

2.1 Beijing case study

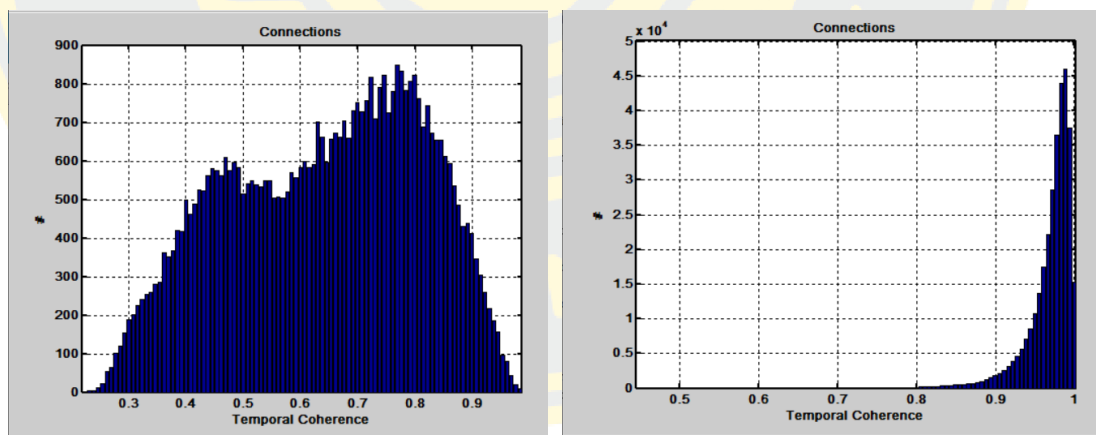
Beijing city case study, the connection with coherence is high. The trend is high to 1, due to the most area is urban there is easily selected stable point as a reference point to connect an interferogram shown as figure 35.



(a)

Figure 35: The connection graph in Beijing city case study with PS analysis

Beijing rural case study, the connection graph in PS analysis is low, with coherence being between 0.3 to 0.7, which only some PS points (greater than 0.7) are used to analyze deformation trends. The connection graph is clearly trended by QPS analysis, with a high threshold going to 1 shown as figure 36.



(a)

(b)

Figure 36: The connection graph in Beijing rural case study. (a) PS analysis, (b) QPS analysis

2.2 Nan case study

Nan case study, a connection graph is inconstant points that appears to two curves, with a high range of 0.9 and a low range of 0.3 by PS analysis. In contrast, the QPS are a high connection of the coherence in each point, with a high threshold of more than 0.9 shown as figure 37.

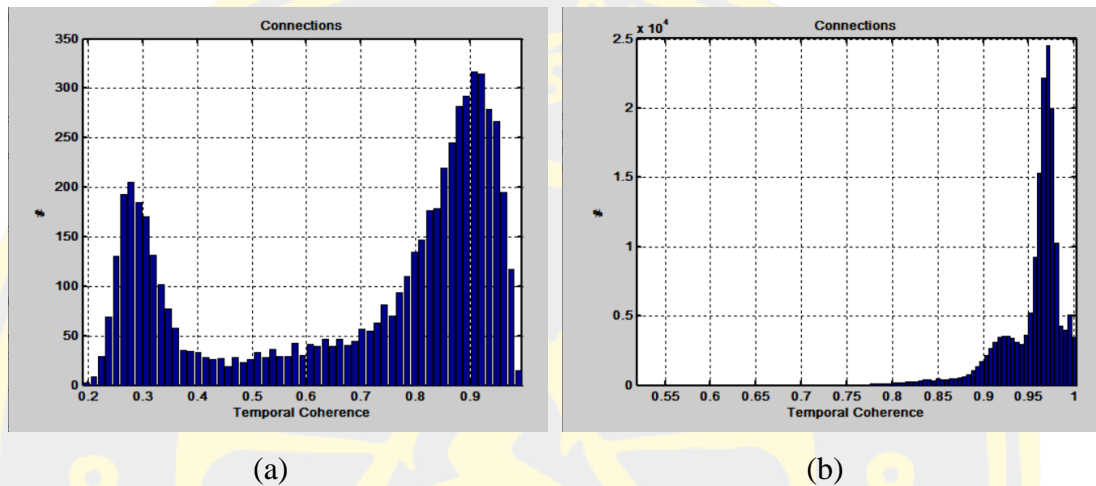


Figure 37: The connection graph in the Nan case study. (a) PS analysis, (b) QPS analysis

CHAPTER V

CONCLUSION AND DISCUSSION

This chapter discusses the successful advance technique of PSI approaches. The work has concentrated on improvement to PS and QPS techniques in the detection of ground displacement and landslide. This chapter discusses more capabilities and limitations that possibilities for further work.

5.1 Conclusion

Persistent Scatterer Interferometry is a very effective technique for land surface monitoring over a wide area, but it is limited by temporal and geometric decorrelation. Therefore, Persistent Scatterer (PS) and Quasi-Persistent Scatterer (QPS) have overcome these problems and become useful for measuring the ground deformation with the high accuracy of a millimeter. Several SAR satellite sensors provides X-band (3.1 cm wavelength), C-band (5.6 cm wavelength), or L-band (23.5 cm wavelength) applied to the different spatial resolutions. The Sentinel-1 was applied for measurement of deformation at a global scale and possible for detect faster varying deformation phenomena. Increase of the potential to discern coherence target within vegetated areas.

This research focused on the ground deformation to the identification of landslide in analyzing the PSI approach using Sentinel-1 SAR images time-series. The PS and QPS were applied to three study sites of urban and rural areas; Nan and two sites of Beijing.

The point was selected as amplitude dispersion index < 0.25 for an urban area, and value < 0.4 for vegetation area. Considering the PSI approach can observe that PS was focused on searching for point-like targets, most of which in urban are gratings, roofs, or roads. A high amplitude dispersion of 0.25 was used for the selection of PS points in Beijing city; the threshold of 0.35 was used for the selection of PS points in Beijing rural and Nan for enhancing generate PS points located surrounding the urban areas. The QPS was a high performance to increase the QPS point. A high amplitude

dispersion of 0.4 was used for the selection of PS points in Beijing rural, and a threshold of 0.45 was used for the selection of PS points in Nan.

5.2 Discussion

The result as the displacement velocity map shows the displacement rate in the LOS direction of the satellite. Displacement observed in each case study is taking between the two acquisitions. The result allows displacement estimation along the most relevant mountain, where clear and large displacement areas can be identified with an average rate of about 30 mm/yr. As a general technique, it observes that the PS works well in an urban area, but it is difficult to apply in a non-urban area where the vegetation cover. PS analysis was relatively high precision and can remove the atmospheric effect most of the time, which was successfully applied to monitoring individual infrastructure in detail, e.g., road, railway shown as figure 38: while unable detected over the non-urban area. In contrast, the QPS was relatively high temporal coherence, even in vegetated and forested areas.

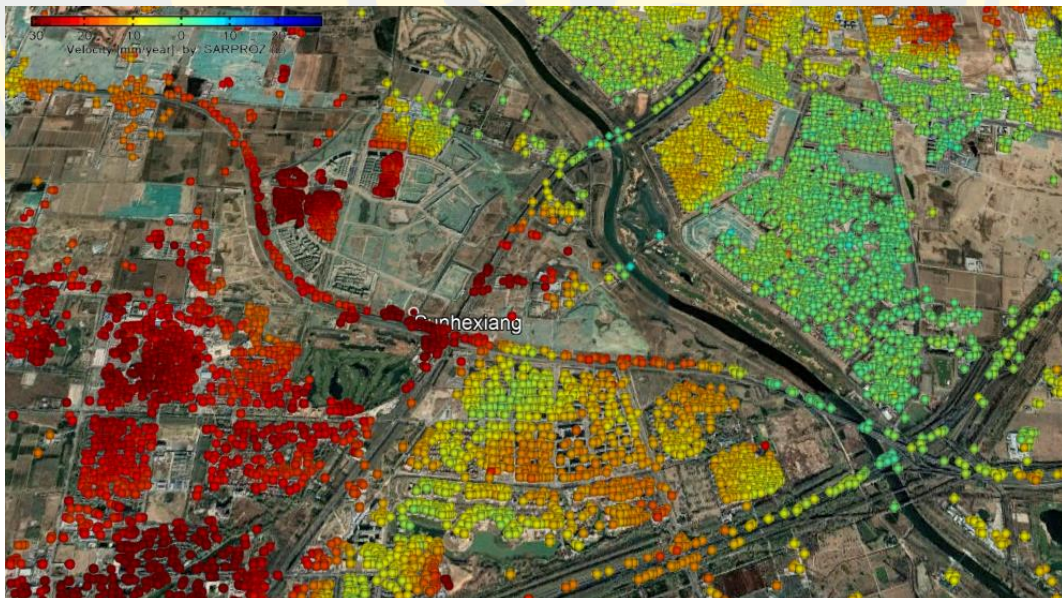


Figure 38: The displacement maps where the road detection with PS analysis in Beijing city case study

The displacement with obvious motion was detected from both PS and QPS, which explains in the movement and easily identifies dangerous areas. The result shows displacement rates in Beijing city, with -99 to 19 mm/yr. There are two obvious

displacements in the eastern part. The susceptible areas of Beijing are related to the geological structure, the density of buildings, the distribution of infrastructure. Displacement map in Nan found that most susceptible areas considered affected by deformation are located on hilltops, and steep valleys. The density of detected points was low in mountainous areas covered by thick vegetation. Both techniques have not improved coherence after graph inversion and APS removal in Nan case study. The deformation velocity obtained using QPS analysis was higher than the PS analysis. This might be that most of the area is covered by both sparsely developed and mostly vegetated. An atmospheric contribution was complicated to evaluate accurately in the areas where the density of a strong scatterer is very low. Thus, the atmospheric contribution to the interferometric phase may not be estimated accurately and removed completely. Although the density QPS points were detected, more noise is a problem in detecting and interpreting the real deformation pattern. Noise is caused by temporal decorrelation, atmospheric errors, errors in topography, or errors in satellite orbits. It is unable to reduce completely there affected the accuracy and analysis of the real deformation.

One landslide in PS and two landslides in QPS were identified in Beijing rural. The landslide without detected points is a small area, located in a valley where no structures as potential good radar targets are reflectance. The landslide types were debris-flow and translational landslide that observed in the Fangshan district. Another landslide in Nan was not detected due to the densely vegetation-covered whole area, such as forests, crops, and perennials. In addition, the sensitivity of these techniques are highly sensitive to the terrain, weather condition, and surface motion that mainly affects to Nan result is not reliable.

The interpretation and prediction of landslides found that more unstable areas and a distinct trend of deformation are preferable results. The landslides were detectable using the QPS but probably undetectable during continuous monitoring with the PS. Also the PS results were usually derived from the advantage of high backscatter and stable phase. Thus, the displacement acquired by PS only referred to PS points, but the QPS can be detected the displacement in the area without PS points. Due to the scatter characteristics of the targets in the earth's surface, and the incidence angle of SAR

acquisitions was not fulfilling the conditions of being of PS points. PS was most likely to acquire information on the deformation trend with QPS results. Therefore, the result of PSI approaches has been found to be highly accurate. A high connection of temporal coherence was generated accurate interferograms; the motion of the surface can be easily detected. The results can serve as useful information for local development planning and decision making.

The research question as formulated in chapter 1 will be answered;

1. How is the ground deformation derived from PSI processing that recognizes stable and unstable areas?

The result was successful using both PS and QPS. The displacement map derived ground deformation velocity rate with millimeter accuracy, which shows the pattern motion in the LOS of satellite direction. This information can be analyzed from several rates and distribution of detected points. The motion between -5 to 5 mm/yr was identified as a stable area (green). The severe displacement was identified to be unstable areas; there were related to the geological structure, the density of building, the distribution of infrastructure. The highest failure can occur in a landslide in the future.

2. How effectiveness is the PSI technique to detect ground deformation in the urban and rural areas?

PS analysis was relatively high precision, which was successfully applied to monitoring urban areas, while unable detected over the non-urban area. The QPS was relatively high precision in an urban area, but low precise even in vegetated and forested areas. Apart from landslide detection, one landslide was identified by PS analysis, while the QPS analysis identified two landslides. These landslides are observed in the Beijing case study. Besides, both techniques were unable to detect the landslide in the Nan case study because in a land characteristic are mainly covered by forests and crops, also the terrain is highly mountain that sensitive with SAR interferometry, so the reasonable deformation of Nan is not an accurate result.

5.3 Limitation and recommendation

The limitation in PS due to poor coherence was not able to obtain meaningful results, especially in a non-urban area. The steep topography and vegetation limited the coherence between successive SAR acquisitions. The coherence along the steep mountain slope was generally poor due to regions affected by layover and shadow. The opposite side is urban areas due to the abundance of constructions which behave like stable scatterers. The geometry of radar images, foreshortening, layover, the shadow might be hinder some detail of this technique. In addition, the exploitation of partially coherence targets was expected to increase the spatial density of detected points and distributed scattering points, especially in rural areas.

Recommendations from this research, we were able to estimate the deformation movement but could not accurately the displacement in Nan. Analyzing the deformation trends is not only focus on trends but also identify possible area to landslide. Using different information from triggering factors and quantify are effectiveness with the displacement time series demonstrates a combination of the rainfall, geological, and morphological, which can be interpreted as preparatory factors to occur the new landslides. Due to PSI analyzing with time series of SAR images made it possible to observe any spatial and temporal changes. However, factors affecting deformation estimations based on these data must be considered, especially in the detection of surface in highly vegetated areas. These factors are included variations in atmospheric conditions and temporal changes due to vegetation between acquisitions. Also, erosion may affect deformation measurement and can be interpreted as subsidence. In addition to the integration of different techniques is significantly advantageous for different monitoring abilities, and which will be useful, such as a Small baseline subset. Lastly, the PSI used the commercial of Sarproz software, processed on Matlab. The results are not easily interpreted; it is challenging to analyze in another GIS environment.

REFERENCES



- Baum, R. L., Galloway, D. L., & Harp, E. L. (2008). Landslide and Land Subsidence Hazards to Pipelines. *Open-File Report 2008-1164*, 192. Retrieved from internal-pdf://69.19.121.70/OF08-1164_508.pdf
- Berardino, P., Fornaro, G., Lanari, R., Member, S., Sansosti, E., & Member, S. (2002). *A New Algorithm for Surface Deformation Monitoring Based on Small Baseline Differential SAR Interferograms*. *40*(11), 2375–2383.
- Bianchini, S., Herrera, G., Mateos, R. M., Notti, D., Garcia, I., Mora, O., & Moretti, S. (2013). Landslide activity maps generation by means of persistent scatterer interferometry. *Remote Sensing*, *5*(12), 6198–6222. <https://doi.org/10.3390/rs5126198>
- Bozzano, F., Mazzanti, P., Perissin, D., Rocca, A., & De Pari, P. (2017). Basin scale assessment of landslides geomorphological setting by advanced InSAR analysis. *Remote Sensing*, *9*(3). <https://doi.org/10.3390/rs9030267>
- Carlà, T., Raspini, F., Intrieri, E., & Casagli, N. (2016). A simple method to help determine landslide susceptibility from spaceborne InSAR data: the Montescaglioso case study. *Environmental Earth Sciences*, *75*(24). <https://doi.org/10.1007/s12665-016-6308-8>
- Chang, C., Yen, J., Hooper, A., Chou, F., & Chen, Y. (2010). *Monitoring of surface deformation in Northern Taiwan using DInSAR and PSInSAR techniques* *Monitoring of Surface Deformation in Northern Taiwan Using DInSAR and PSInSAR Techniques*. *01*(October 2014). [https://doi.org/10.3319/TAO.2009.11.20.01\(TH\)1](https://doi.org/10.3319/TAO.2009.11.20.01(TH)1).
- Chen, H., Wang, Y., Zhang, Y., Yan, Y., Avenue, X., & Zone, W. H. (2018). SURFACE DEFORMATION OF KANGDING AIRPORT , QINGHAI-TIBET PLATEAU , CHINA USING INSAR TECHNIQUES AND MULTI-TEMPORAL SENTINEL-1 DATASETS School of Resources and Environment University of Electronic Science and Technology of China (UESTC) Department of Geog. *IGARSS 2018 - 2018 IEEE International Geoscience and Remote Sensing Symposium*, 3067–3070.
- Chen, M., Tomás, R., Li, Z., Motagh, M., Li, T., & Hu, L. (2016). *Imaging Land Subsidence Induced by Groundwater Extraction in Beijing (China) Using Satellite Radar Interferometry*. 1–21. <https://doi.org/10.3390/rs8060468>
- Chen, M., Tomás, R., Li, Z., Motagh, M., Li, T., Hu, L., ... Gong, X. (2016). Imaging land subsidence induced by groundwater extraction in Beijing (China) using satellite radar interferometry. *Remote Sensing*, *8*(6), 1–21. <https://doi.org/10.3390/rs8060468>

- Ciampalini, A., Bardi, F., Bianchini, S., Frodella, W., del Ventisette, C., Moretti, S., & Casagli, N. (2014). Analysis of building deformation in landslide area using multisensor PSInSARTM technique. *International Journal of Applied Earth Observation and Geoinformation*, 33(1), 166–180. <https://doi.org/10.1016/j.jag.2014.05.011>
- Ciampalini, A., Raspini, F., Frodella, W., Bardi, F., Bianchini, S., & Moretti, S. (2016). The effectiveness of high-resolution LiDAR data combined with PSInSAR data in landslide study. *Landslides*, 13(2), 399–410. <https://doi.org/10.1007/s10346-015-0663-5>
- Ciampalini, A., Raspini, F., Lagomarsino, D., Catani, F., & Casagli, N. (2016). Landslide susceptibility map refinement using PSInSAR data. *Remote Sensing of Environment*, 184, 302–315. <https://doi.org/10.1016/j.rse.2016.07.018>
- Crosetto, M., Monserrat, O., & Budillon, A. (2019). Urban Deformation Monitoring using Persistent Scatterer Interferometry and SAR tomography. In *Urban Deformation Monitoring using Persistent Scatterer Interferometry and SAR tomography*. <https://doi.org/10.3390/books978-3-03921-127-2>
- Crosetto, M., Monserrat, O., Cuevas-González, M., Devanthery, N., & Crippa, B. (2016). Persistent Scatterer Interferometry: A review. *ISPRS Journal of Photogrammetry and Remote Sensing*, 115, 78–89. <https://doi.org/10.1016/J.ISPRSJPRS.2015.10.011>
- Dehghani, M., & Javadi, H. R. (2013). Remote sensing of ground deformation. *SPIE Newsroom*, (June 2014), 2–5. <https://doi.org/10.1117/2.1201303.004772>
- Del, M., & Idrogeologico, R. (2012). *Landslides forecasting analysis by displacement time series*. 2011(January), 19–23.
- Ding, X. L., Liu, G. X., Li, Z. W., Li, Z. L., & Chen, Y. Q. (2004). Ground subsidence monitoring in Hong Kong with satellite SAR interferometry. *Photogrammetric Engineering and Remote Sensing*, 70(10), 1151–1156. <https://doi.org/10.14358/PERS.70.10.1151>
- Duro, J., Iglesias, R., Blanco, P., Sánchez, F., & Albiol, D. (2015). Improved PSI performance for landslide monitoring applications. *European Space Agency, (Special Publication) ESA SP, SP-731*(June). <https://doi.org/10.5270/fringe2015.pp299>
- Emardson, T. R., Simons, M., & Webb, F. H. (2003). Neutral atmospheric delay in interferometric synthetic aperture radar applications: Statistical description and mitigation. *Journal of Geophysical Research: Solid Earth*, 108(B5), 1–8. <https://doi.org/10.1029/2002jb001781>

- Ferretti, A., Prati, C., & Rocca, F. (1999). Permanent scatterers in SAR interferometry. *International Geoscience and Remote Sensing Symposium (IGARSS)*, 3(1), 1528–1530.
- Ferretti, Alessandro, Colesanti, C., Perissin, D., Prati, C., & Rocca, F. (2004). Evaluating the effect of the observation time on the distribution of sar permanent scatterers. *European Space Agency, (Special Publication) ESA SP*, (550), 167–172.
- Ferretti, Alessandro, Prati, C., & Rocca, F. (2001). Permanent scatterers in SAR interferometry. *IEEE Transactions on Geoscience and Remote Sensing*, 39(1), 8–20. <https://doi.org/10.1109/36.898661>
- Fiaschi, S., Holohan, E. P., Sheehy, M., & Floris, M. (2019). PS-InSAR analysis of Sentinel-1 data for detecting ground motion in temperate oceanic climate zones: A case study in the Republic of Ireland. *Remote Sensing*, 11(3). <https://doi.org/10.3390/rs11030348>
- Francisca, F. L. I., & Javier, F. I. F. (2015). *Human-induced coastal landslide reactivation . Monitoring by PSInSAR techniques and urban damage survey (SE Spain)* *Human-induced coastal landslide reactivation . Monitoring by PSInSAR techniques and urban damage survey (SE Spain)*. (October). <https://doi.org/10.1007/s10346-015-0612-3>
- Gao, J., & Sang, Y. (2017). Identification and estimation of landslide-debris flow disaster risk in primary and middle school campuses in a mountainous area of Southwest China. *International Journal of Disaster Risk Reduction*, 25, 60–71. <https://doi.org/10.1016/J.IJDRR.2017.07.012>
- Gao, M., Gong, H., Li, X., Chen, B., Zhou, C., Shi, M., ... Duan, G. (2019). Land subsidence and ground fissures in Beijing Capital International Airport (BCIA): Evidence from Quasi-PS InSAR analysis. *Remote Sensing*, 11(12). <https://doi.org/10.3390/rs11121466>
- Greif, V., & Vlcko, J. (2013). Landslide Science and Practice. *Landslide Science and Practice*, (July 2015). <https://doi.org/10.1007/978-3-642-31445-2>
- Guzzetti, F., Manunta, M., Ardizzone, F., Pepe, A., Cardinali, M., Zeni, G., ... Lanari, R. (2009). Analysis of ground deformation detected using the SBAS-DInSAR technique in Umbria, Central Italy. *Pure and Applied Geophysics*, 166(8–9), 1425–1459. <https://doi.org/10.1007/s00024-009-0491-4>
- Heimlich, C., Gourmelen, N., Masson, F., Schmittbuhl, J., Kim, S. W., & Azzola, J. (2015). Uplift around the geothermal power plant of Landau (Germany) as observed by InSAR monitoring. *Geothermal Energy*, 3(1).

<https://doi.org/10.1186/s40517-014-0024-y>

- Hilley, G. E., Bürgmann, R., Ferretti, A., Novali, F., & Rocca, F. (2004). Dynamics of slow-moving landslides from permanent scatterer analysis. *Science*, *304*(5679), 1952–1955. <https://doi.org/10.1126/science.1098821>
- Hooper, A., Segall, P., & Zebker, H. (2007). Persistent scatterer interferometric synthetic aperture radar for crustal deformation analysis, with application to Volcán Alcedo, Galápagos. *Journal of Geophysical Research: Solid Earth*, *112*(7), 1–21. <https://doi.org/10.1029/2006JB004763>
- Hooper, Andrew, Zebker, H., Segall, P., & Kampes, B. (2004). A new method for measuring deformation on volcanoes and other natural terrains using InSAR persistent scatterers. *Geophysical Research Letters*, *31*(23), 1–5. <https://doi.org/10.1029/2004GL021737>
- Höser, T. (2018). *Analysing the Capabilities and Limitations of InSAR using Sentinel-1 data for Landslide Detection and Monitoring*. (July), 104. Retrieved from https://www.researchgate.net/profile/Thorsten_Hoeser/publication/327939547_Analysing_the_Capabilities_and_Limitations_of_InSAR_using_Sentinel-1_Data_for_Landslide_Detection_and_Monitoring/links/5bae2c1e299bf13e60525c1c/Analysing-the-Capabilities-and-Limit
- Kincal, C., Li, Z., Drummond, J., Liu, P., Hoey, T., & Muller, J.-P. (2017). Landslide Susceptibility Mapping Using GIS-based Vector Grid File (VGF) Validating with InSAR Techniques: Three Gorges, Yangtze River (China). *AIMS Geosciences*, *3*(1), 116–141. <https://doi.org/10.3934/geosci.2017.1.116>
- Kuri, M., Arora, M. K., & Sharma, M. L. (2018). Slope stability analysis in nainital town using PS and QPS InSAR technique. *International Geoscience and Remote Sensing Symposium (IGARSS)*, *2018-July*, 4443–4446. <https://doi.org/10.1109/IGARSS.2018.8517713>
- Laat, R. Van Der. (1996). *Ground-Deformation Methods and Results*.
- Lagios, E., Sakkas, V., Novali, F., Bellotti, F., Ferretti, A., Vlachou, K., & Dietrich, V. (2013). Tectonophysics SqueeSAR™ and GPS ground deformation monitoring of Santorini Volcano (1992 – 2012): Tectonic implications. *Tectonophysics*, *594*(February 2012), 38–59. <https://doi.org/10.1016/j.tecto.2013.03.012>
- Lazecky, M., Comut, F. C., Bakon, M., Qin, Y., Perissin, D., Hatton, E., ... Ustun, A. (2016). Concept of an Effective Sentinel-1 Satellite SAR Interferometry System. *Procedia Computer Science*, *100*(October), 14–18. <https://doi.org/10.1016/j.procs.2016.09.118>

- Luo, Q., Perissin, D., Dogan, O., Lin, H., & Wang, W. (2012). Tianjin suburbs PS-QPS analysis and validation with leveling data. *International Geoscience and Remote Sensing Symposium (IGARSS)*, 3915–3918. <https://doi.org/10.1109/IGARSS.2012.6350556>
- Massonnet, D., & Feigl, K. L. (1998). Radar interferometry and its application to changes in the earth's surface. *Reviews of Geophysics*, 36(4), 441–500. <https://doi.org/10.1029/97RG03139>
- Mi, S. J., Li, Y. T., Wang, F., Li, L., Ge, Y., Luo, L., ... Chen, J. B. (2017). A research on monitoring surface deformation and relationships with surface parameters in Qinghai Tibetan Plateau permafrost. *International Archives of the Photogrammetry, Remote Sensing and Spatial Information Sciences - ISPRS Archives*, 42(2W7), 629–633. <https://doi.org/10.5194/isprs-archives-XLII-2-W7-629-2017>
- Nathan, A. J., & Scobell, A. (2012). Data interpretation and error analysis. In *Foreign Affairs* (Vol. 91). <https://doi.org/10.1017/CBO9781107415324.004>
- Nengwu, M., Weiyan, C., Shuangping, L., Min, Z., Ping, H., Zonghuang, J., ... Tao, L. (2012). Landslide monitoring by PS-InSAR along Qing river. *Proceedings of the 2nd International Workshop on Earth Observation and Remote Sensing Applications, EORSA 2012*, (2), 235–239. <https://doi.org/10.1109/EORSA.2012.6261172>
- Notti, D., Meisina, C., & Zucca, F. (2009). Analysis of PSInSARTM data for landslide studies from regional to local scale. ... of *ESA Fringe 2009 Workshop, Frascati, 2009*(March). Retrieved from http://earth.eo.esa.int/workshops/fringe09/proceedings/papers/p2_40nott.pdf
- Oliveira, S. C., Zêzere, J. L., Catalão, J., & Nico, G. (2015). The contribution of PSInSAR interferometry to landslide hazard in weak rock-dominated areas. *Landslides*, 12(4), 703–719. <https://doi.org/10.1007/s10346-014-0522-9>
- Osmanoğlu, B., Sunar, F., Wdowinski, S., & Cabral-Cano, E. (2016). Time series analysis of InSAR data: Methods and trends. *ISPRS Journal of Photogrammetry and Remote Sensing*, 115, 90–102. <https://doi.org/10.1016/j.isprsjprs.2015.10.003>
- Otukei, J., Atolere, P., Gidudu, A., & Martini, F. (2019). Ground Deformation Assessment of the Albertine Graben Using Insar. *South African Journal of Geomatics*, 8(2), 130–143. <https://doi.org/10.4314/sajg.v8i2.2>
- Patrascu, C., Popescu, A. A., & Datcu, M. (2016). Comparative assessment of multi-temporal InSAR techniques for generation of displacement maps: A case study for Bucharest area. *UPB Scientific Bulletin, Series C: Electrical Engineering and*

- Computer Science*, 78(2), 135–146.
- Perissin, D., & Rocca, F. (2006). High-accuracy urban DEM using permanent scatterers. *IEEE Transactions on Geoscience and Remote Sensing*, 44(11), 3338–3347. <https://doi.org/10.1109/TGRS.2006.877754>
- Perissin, D., & Wang, T. (2011). Time-Series InSAR Applications Over Urban Areas in China. *IEEE Journal of Selected Topics in Applied Earth Observations and Remote Sensing*, 4(1), 92–100. <https://doi.org/10.1109/JSTARS.2010.2046883>
- Perissin, D., & Wang, T. (2012). Repeat-Pass SAR Interferometry With Partially Coherent Targets. *IEEE Transactions on Geoscience and Remote Sensing*, 50(1), 271–280. <https://doi.org/10.1109/TGRS.2011.2160644>
- Perissin, D., Wang, Z., Prati, C., & Rocca, F. (2013a). Terrain monitoring in China via ps-qps insar: Tibet and the three gorges dam. *European Space Agency, (Special Publication) ESA SP, 704 SP*(January).
- Perissin, D., Wang, Z., Prati, C., & Rocca, F. (2013b). Terrain monitoring in China via ps-qps insar: Tibet and the three gorges dam. *European Space Agency, (Special Publication) ESA SP, 704 SP*, 2–6.
- Plain, P., Emilia, P., Antonielli, B., Monserrat, O., Bonini, M., Cenni, N., ... Sani, F. (2016). *Persistent Scatterer Interferometry analysis of ground deformation*. 1440–1455. <https://doi.org/10.1093/gji/ggw227>
- Razi, P., Sumantyo, J. T. S., Perissin, D., & Kuze, H. (2018). Long-Term Land Deformation Monitoring Using Quasi-Persistent Scatterer (Q-PS) Technique Observed by Sentinel-1A: Case Study Kelok Sembilan. *Advances in Remote Sensing*, 07(04), 277–289. <https://doi.org/10.4236/ars.2018.74019>
- Roque, D., Fonseca, A. M., Henriques, M. J., & Falcão, A. P. (2014). A First Approach for Displacement Analysis in Lisbon Downtown Using PS-InSAR. *Procedia Technology*, 16, 288–293. <https://doi.org/10.1016/j.protcy.2014.10.094>
- Rosen, P. A. (2000). Synthetic aperture radar interferometry. *Proceedings of the IEEE*, 88(3), 333–380. <https://doi.org/10.1109/5.838084>
- Safari, A., Gamse, S., & Seyedrezaei, M. (2018). *Space-Based Monitoring of Ground Deformation Space-Based Monitoring of Ground Deformation*. (June).
- Tofani, V., Raspini, F., Catani, F., & Casagli, N. (2014). Persistent scatterer interferometry (PSI) technique for landslide characterization and monitoring. *Landslide Science for a Safer Geoenvironment: Volume 2: Methods of Landslide Studies*, 351–357. https://doi.org/10.1007/978-3-319-05050-8_55
- Vant, M. R. (1989). Synthetic aperture radar signal processing. *Onde Electrique*, 69(6),

45–57.

- Vöge, M., Frauenfelder, R., Ekseth, K., Arora, M. K., Bhattacharya, A., & Bhasin, R. K. (2015). The use of SAR interferometry for landslide mapping in the Indian Himalayas. *International Archives of the Photogrammetry, Remote Sensing and Spatial Information Sciences - ISPRS Archives*, 40(7W3), 857–863. <https://doi.org/10.5194/isprsarchives-XL-7-W3-857-2015>
- Wang, T., Liao, M., Tang, J., Perissin, D., Rocca, F., & Rucci, A. (2010). Landslides monitoring over the three Gorges region with C- and X-band InSar data. *European Space Agency, (Special Publication) ESA SP*, 684 SP(October).
- Yang, Q., Ke, Y., Zhang, D., Chen, B., Gong, H., Lv, M., ... Li, X. (2018). Multi-scale analysis of the relationship between land subsidence and buildings: A case study in an eastern Beijing Urban Area using the PS-InSAR technique. *Remote Sensing*, 10(7). <https://doi.org/10.3390/rs10071006>
- Yarmohammad Touski, M., Veiskarami, M., & Dehghani, M. (2019). Interferometric Point Target Analysis (Ipta) for Landslide Monitoring. *ISPRS - International Archives of the Photogrammetry, Remote Sensing and Spatial Information Sciences*, XLII-4/W18(October), 1079–1083. <https://doi.org/10.5194/isprs-archives-xlii-4-w18-1079-2019>
- Zebker, H. A., & Villasenor, J. (2007). *Zebker, Villasenor_1992_Decorrelation in Interferometric Radar Echoes*. (818), 1–19.
- Zhang, W., Wang, W., & Xia, Q. (2012). *Energy Procedia Landslide Risk Zoning Based on Contribution Rate Weight Stack Method*. <https://doi.org/10.1016/j.egypro.2012.01.030>
- Zhou, K., Wang, F., Wang, M., & Ding, Q. (2019). Land surface deformation monitoring of the songyuan langya dam using mt-InSAR. *2019 SAR in Big Data Era, BIGSAR DATA 2019 - Proceedings*, (2001), 1–4. <https://doi.org/10.1109/BIGSAR DATA.2019.8858452>
- Zhou, X., Chang, N. Bin, & Li, S. (2009). Applications of SAR interferometry in earth and environmental science research. *Sensors*, 9(3), 1876–1912. <https://doi.org/10.3390/s90301876>

BIOGRAPHY

NAME NATTIYA KORAWAT

DATE OF BIRTH 23 Nov 1993

PLACE OF BIRTH Bangkok

PRESENT ADDRESS 50/238 Prueksa 57, Khukot, Lamlukka, Patumthani, 12130

